NAVAL POSTGRADUATE SCHOOL

Monterey, California

VISCOELASTIC ANALYSIS METHOD FOR
ROCKET MOTORS CONTAINING CRACKS

BY

Gerald H. Lindsey

March 1973

Approved for public release, distribution unlimited.

NAVAL POSTGRADUATE SCHOOL
Monterey, California

Rear Admiral Mason Freeman, USN
Superintendent

Milton U. Clauser
Provost

ABSTRACT

The basic definitions for viscoelastic stress intensity factors are set forth with associated computations for determining them in laboratory specimens. Laboratory tests have been conducted to characterize propellants fracturewise, and the most suitable test found was the long strip subjected to a constant force loading. The influence of dewetting on the fracture characterization appears to be significant, but the matter has not yet been fully resolved.

An approximate method for performing viscoelastic fracture analyses has been presented which incorporates the fore-mentioned fracture characterization. It requires minimum computer usage and should yield good results.

TABLE OF CONTENTS

VISCOELASTIC ANALYSIS METHOD FOR ROCKET MOTORS CONTAINING CRACKS

INTRODUCTION

Solid propellant has been found to be susceptible to cracking during fabrication or service just like other engineering materials. The cracks may or may not be detrimental to the rocket motor depending upon location, size, and propagation rate; however a potential danger always exists when a crack is present; for instance, the crack introduces additional burning which may cause significant overpressure and a subsequent malfunction. It is also possible that a crack may create a pathway for burning to the case prematurely, producing a burn-through. On the other hand, it may lead to other areas of the grain where malfunctioning occurs due to alterations in the ballistics or due to loss of structural integrity resulting from the high stresses and strains associated with the crack front exceeding the design limits. The consequences of such developments must be determined for each individual situation; therefore a theoretical basis for predicting the initiation and propagation behavior of cracks in propellant is needed.

The elastic theory of fracture mechanics has been successfully applied to rocket motor geometries and loadings by Francis, Lindsey and Parmerter (1). Similar work was done on viscoelastic materials by Francis et al (2) using an unfilled polyurethane for the grain material. Two-dimensional grain cross-sectional slices containing cracks were analyzed and compared with experiment. Predictions of viscoelastic crack behavior were made by using a sequence of elastic crack propagation problems. The method of fracture characterization followed that used by Knauss (3) on the same polyurethane material. Progress was made and results of the study were used to provide guidelines for some of the concepts developed in this work.

In this report the fundamental expressions for stress and displacement near a crack tip are developed for linear, unfilled, viscoelastic materials. These expressions are used to reduce crack propagation data obtained on strips of propellant that are considered to be infinite in extent. Both constant stress and constant displacement boundary conditions are employed in the tests for purposes of comparison. Experimental fracture characterization in terms of stress intensity factors versus crack velocity in propellant is the end result. Finally a method is presented for the viscoelastic analysis of rocket motors containing initial cracks.

DEFINITIONS AND ASSUMPTIONS

Stress Intensity Factor

Elastic solutions for the stress field in the vicinity of a crack by Williams[4], Westergaard[5] and Irwin[6] have been written in terms of undetermined coefficients that became explicit when the particular body geometry and loading are specified. In terms of the mixed coordinates (see Fig. 1)

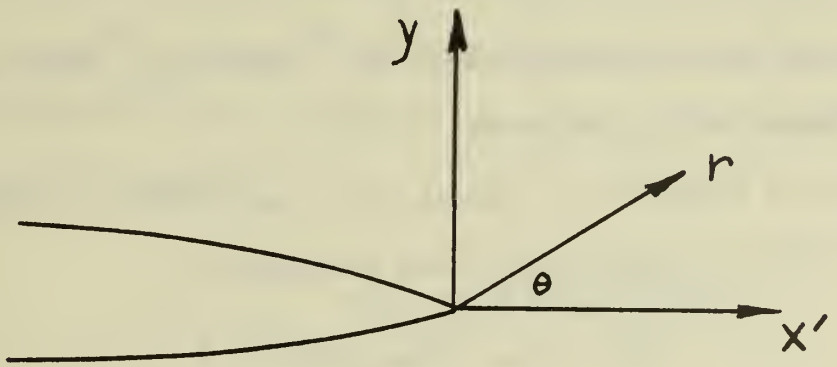

Figure 1 Stationary crack coordinate system.

normally used to express the stress field,

$$\sigma_{ij}(r,\theta) = \frac{K_1}{\sqrt{2r}} f_{ij}(\theta) + \frac{K_2}{\sqrt{2r}} g_{ij}(\theta) \qquad (1)$$

where K_1 and K_2 are the opening mode and shearing mode stress intensity factors (S.I.F.) respectively.

To more precisely define these quantities, use can be made of the opening and shearing stresses in expanded form.

$$\sigma_y(r,\theta) = \frac{K_1}{\sqrt{2r}} \operatorname{Cos}\frac{\theta}{2}\left[1 + \operatorname{Sin}\frac{\theta}{2}\operatorname{Sin}\frac{3\theta}{2}\right] + \frac{K_2}{\sqrt{2r}} \operatorname{Sin}\frac{\theta}{2}\operatorname{Cos}\frac{\theta}{2}\operatorname{Cos}\frac{3\theta}{2} \qquad (2a)$$

$$\tau_{xy}(r,\theta) = \frac{K_1}{\sqrt{2r}} \operatorname{Sin}\frac{\theta}{2} \operatorname{Cos}\frac{\theta}{2} \operatorname{Cos}\frac{3\theta}{2} + \frac{K_1}{\sqrt{2r}} \operatorname{Cos}\frac{\theta}{2}\left[1 - \operatorname{Sin}\frac{\theta}{2} \operatorname{Sin}\frac{3\theta}{2}\right] \qquad (2b)$$

These two stress components possess a certain assymetry, and the S.I.F. can be conveniently defined in terms of them.

$$K_1 \equiv \lim_{r \to 0} \sqrt{2r}\, \sigma_y(r,0) \qquad (3a)$$

$$K_2 \equiv \lim_{r \to 0} \sqrt{2r}\, \tau_{xy}(r,0) \qquad (3b)$$

where the limit is used to indicate that this relationship only applies in a small neighborhood of the crack-tip.

For $\theta = 0$, $r = x'$ and $y = 0$. Making this substitution, the definition can be written also in terms of cartesian coordinates.

$$K_1 \equiv \lim_{x \to 0} \sqrt{2x'}\, \sigma_y(x';0) \qquad (4a)$$

$$K_2 \equiv \lim_{x \to 0} \sqrt{2x'}\, \tau_{xy}(x';0) \qquad (4b)$$

In viscoelastic fracture no standard definitions of stress intensity factor, fracture toughness, coordinate orientation, etc. have emerged; however it appears straight forward to extend the above definitions in the obvious way. Since the crack is normally propagating under load in viscoelastic materials, it is convenient to shift the base of reference to the system shown in Fig. 2.

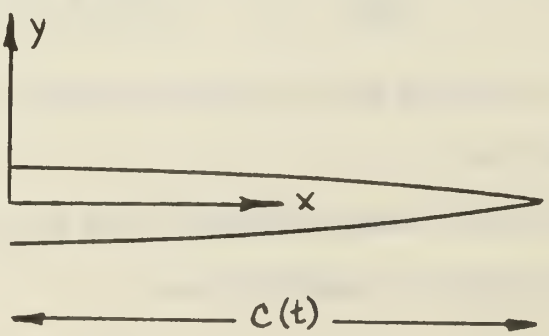

Figure 2 Moving crack coordinate system.

Translating the previous expressions for S.I.F. by an amount c(t) and allowing for the possibility of the stresses varying with time,

$$K_1^v(t) \equiv \lim_{x \to c(t)} \{[2(x - c(t))]^{\frac{1}{2}} \sigma_y(x,0,t)\} \tag{5a}$$

$$K_2^v(t) \equiv \lim_{x \to c(t)} \{[2(x - c(t))]^{\frac{1}{2}} \tau_{xy}(x,0,t)\} \tag{5b}$$

Apart from the square-root-of-two factor, this definition is the same as used by Graham[7]. Knauss[8] also used this form, but Meuller[9] and Knauss and Meuller[10] used a nondimensional form of the above for an infinite strip of width 2b.

$$I \equiv \lim_{x \to c(t)} \left\{\left[\frac{x - c(t)}{b}\right]^{\frac{1}{2}} \frac{\sigma_y(x,0,t)}{\sigma_o}\right\} \tag{6}$$

Since all of these forms are closely related, and since the definitions of equation (5) possess the appropriate limit check for elastic materials, they will be used throughout this report.

Fracture Postulate

Fracture studies in recent years have led to the conclusion that flaws in materials will grow when under load. This continues until the flaw becomes of critical size, at which time the specimen undergoes unstable crack propagation and fracture. This has been found to be true for metals, especially in fatigue, and for nonmetals alike.

Knauss[8] has published theoretical developments of these ideas for viscoelastic materials and has shown that the important parameter of interest for rate sensitive materials is crack velocity. In the elastic case, the threshold of rapid crack propagation is often the focus of interest; however in viscoelastic materials the crack is found to propagate

for almost any load level. The velocities are infinitesimally small for low loads and increase as the body is more highly stressed. The question to be answered then becomes, not at what load level does the crack propagate, but at what velocity does the crack propagate for any given load. As defined, the viscoelastic stress intensity factor contains information relative to the specimen geometry, material and boundary conditions; therefore we desire the relationship between stress intensity factor and crack velocity.

This brings us to the fracture postulate:

If $$[K_1^v(t)]_{\text{Body 1}} = [K_1^v(t)]_{\text{Body 2}}$$

then $$[\dot{c}(t)]_{\text{Body 1}} = [\dot{c}(t)]_{\text{Body 2}}$$

In words this states that for every stress intensity factor there is a corresponding unique crack velocity.

Knauss [3] has performed experiments on Solithane 113, a polyurethane elastomer, which have substantiated this to a degree (Francis et al[2] have duplicated these tests and done additional work on other types of loads.) For all temperature ranges tested, the material was elastic in the sense that it did not relax; however the crack behavior was viscoelastic and exhibited a velocity that varied with loading. Knauss postulates that in this type of material, when the strain at the crack tip is the same in two different bodies, the same crack velocity will be produced. Of course in a body that is behaving elastically so far as stress and strain are concerned, the same strain level is equivalent to the same stress intensity factor. Thus, in the postulate of fracture, we are following the previous ideas of Knauss. Furthermore, it states that if the stress intensity factor history can be calculated, the crack velocity equation can be determined

from the experimental characterization of the material. Once this is known, the crack history for a rocket motor can be obtained. This will be demonstrated later.

EXACT SOLUTIONS FOR S.I.F.

The classical correspondence principle normally applied in the solution of boundary value problems in the linear, quasi-static theory of viscoelasticity, does not apply for crack propagation problems. In this instance new boundary is being created as the crack propagates, and the conditions on the boundary are changing in type; i.e. at the crack tips they are changing from displacement to stress boundary conditions and vice versa. In this kind of problem there will be points of the boundary where only partial histories of the boundary conditions are known a priori; consequently the integral Laplace Transform cannot be computed, and the correspondence principle is not applicable.

Graham[11] has extended the correspondence principle to encompass crack problems. Two examples that are of particular interest in fracture characterization of propellant are the long strip with either displacement or stress boundary conditions.

Long Strip with Stress Boundary Conditions

The sheet and loading are symmetric about the x axis, as shown in Fig. 3, where the lower half of the stip is removed and replaced by the stresses which act along the sheet's horizontal centerline.

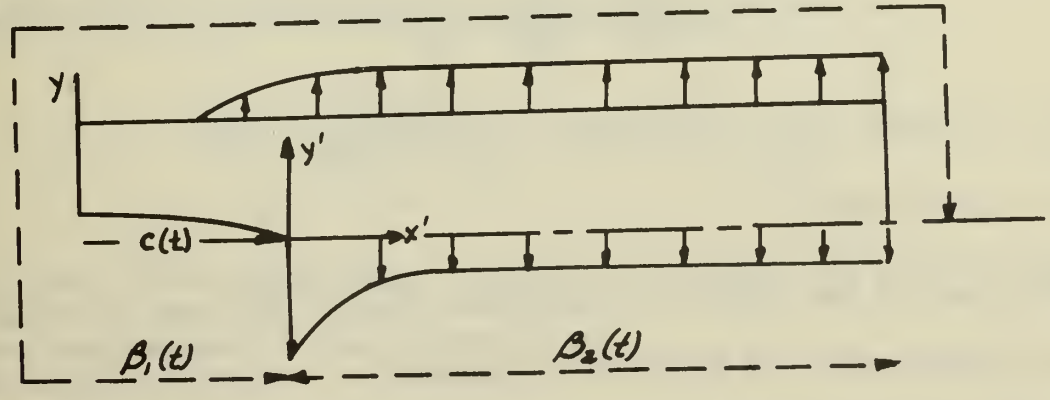

Fig 3. Constant Stress Sheet

Let the entire boundary of the sheet be defined as β with $\beta_2(t)$ representing the uncracked portion of the x-axis and $\beta_1(t)$ representing the remaining boundary. Then $\beta = \beta_1(t) \cup \beta_2(t)$. The boundary conditions are:

$$\begin{aligned} \sigma_s(X,t) &= 0 && && \text{on } \beta \\ \sigma_n(X,t) &= \begin{cases} 0 & \text{on crack edge} \\ 0 & \text{on } x = 0,L \\ \sigma_a(X,t) & \text{on } y = b \end{cases} && \text{on } \beta_1(t) \\ u_n(X,t) &= 0 && && \text{on } \beta_2(t) \end{aligned} \tag{7}$$

the subscripts s and n respectively refer to normal and shear components. The boundary conditions of Equation (7) meet the criteria of Graham's extended correspondence principle. The extended correspondence principle permits the construction of the viscoelastic solution for a moving crack from an elastic solution for a moving crack.

$$\sigma_{ij}^{v}(t) = L^{-1}\left[\sigma_{ij}^{me*}(s)\right] \begin{matrix} E \to E^* \\ \upsilon \to \upsilon^* \end{matrix} \tag{8}$$

where m designates a moving crack. The moving crack solution may be generated from a similar stationary elastic crack solution. For an incompressible elastic strip, the stresses in the neighborhood of the crack tip are given by,

$$\sigma_{ij}^{e} = \frac{\sigma\sqrt{b}}{\sqrt{2r\pi}} f_{ij}(\theta) \tag{9}$$

where σ = boundary stress in uniform stress region

2b = strip width

The crack is now imagined to propagate slowly. For most elastomers and all propellants, the velocity of propagation is quite low, which makes the inertial terms in the equations of motion small and negligible. The

field equations become the same as those of the static crack problem; therefore the stress field is the same as that given in Equation (9), except that the coordinate system to which the above quantities are referenced is now moving since it is attached to the crack tip. The dynamic, elastic solution is

$$\overset{me}{\sigma}_{ij}(t) = \frac{\sigma(t)\sqrt{b}}{\sqrt{2\pi r(t)}} f_{ij}[\theta(t)] \tag{10}$$

It is a simple matter to reference these quantities to an inertial coordinate system. As stated previously the loading and geometry is taken such that only the opening mode of propagation is present; therefore from Fig. 2

$$r(t) \cdot \cos\theta(t) + c(t) = x \tag{11}$$

Equation (10) for the dynamic elastic problem becomes,

$$\overset{me}{\sigma}_{ij}(t) = \frac{\sigma(t)\sqrt{b}}{\sqrt{2\pi(x - c(t)}} F_{ij}[\theta(t)] \tag{12}$$

To use the correspondence principle, the transform of Equation (12) is needed.

$$\overset{me*}{\sigma}_{ij} = \left[\frac{\sigma(t)\sqrt{b}}{\sqrt{2\pi[x - c(t)]}} F_{ij}[\theta(t)] \right]^{*} \tag{13}$$

By Equation (8), the corresponding viscoelastic expression is

$$\sigma^{v*}_{ij} = \left[\frac{\sigma(t)\sqrt{b}}{\sqrt{2\pi[x - c(t)]}} F_{ij}[\theta(t)]\right]^{*}_{\substack{E \to E^* \\ \nu \to \nu^*}} \tag{14}$$

Since E and ν do not appear, the inversion is trivial, and the viscoelastic stresses are identical to the elastic ones.

$$\sigma_{ij}^{v}(t) = \frac{\sigma(t)\sqrt{b}}{\sqrt{2\pi(x - c(t))}} F_{ij}[\theta(t)] \tag{15}$$

From this result and by application of the definition of stress intensity factor given in Equation (5),

$$K_1^{v}(t) = \sigma(t)\sqrt{\frac{b}{\pi}} \tag{16}$$

This viscoelastic solution is accurate to the degree that the elastic solution from which it was constructed is accurate. In this case it is known to be good via Knauss'[12] series solution.

Long Strip with Displacement Boundary Conditions

Many elastic crack propagation studies have been conducted on strips with displacement boundary conditions, but in order to use it for viscoelastic fracture, the viscoelastic solution is needed. This is not directly obtainable from Graham, but it is possible to generate it by following some of Graham's methods.

Consider the viscoelastic boundary value problem of Fig. 4, where A, B, and C do not involve material constants, and the crack is propagating.

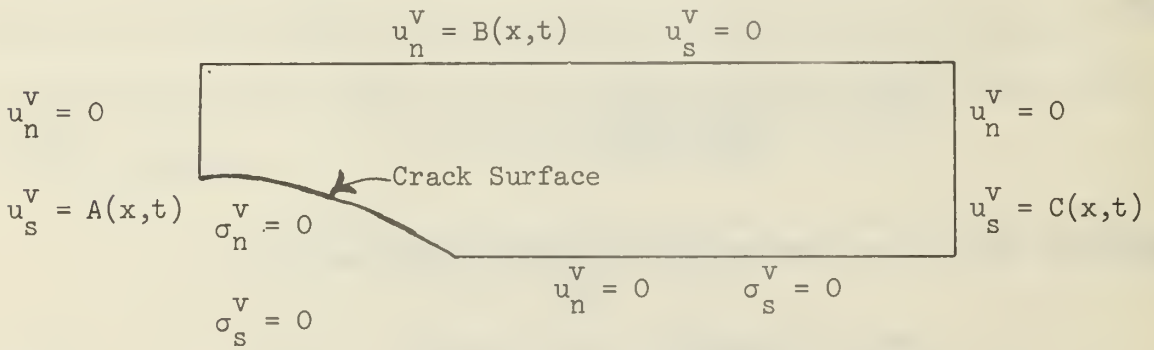

Fig. 4 Viscoelastic problem.

Following Graham, we consider a dynamic elastic problem with a moving crack and the same boundary conditions. This is shown in Fig. 5.

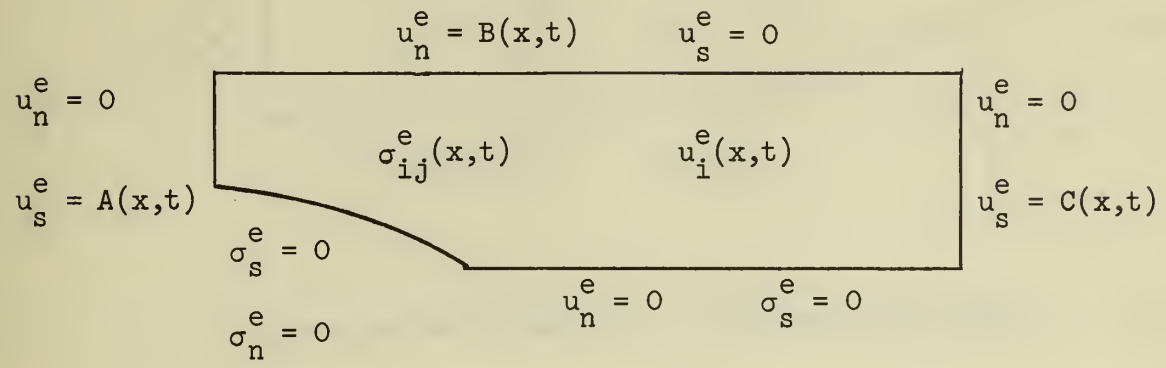

Fig. 5 Elastic problem.

The solution to this problem, $\sigma_{ij}^e(x,t)$ and $u_i^e(x,t)$ is known, and with it, all field quantities can be computed on the boundary. This solution allows us to define the equivalent elastic problem shown in Fig. 6.

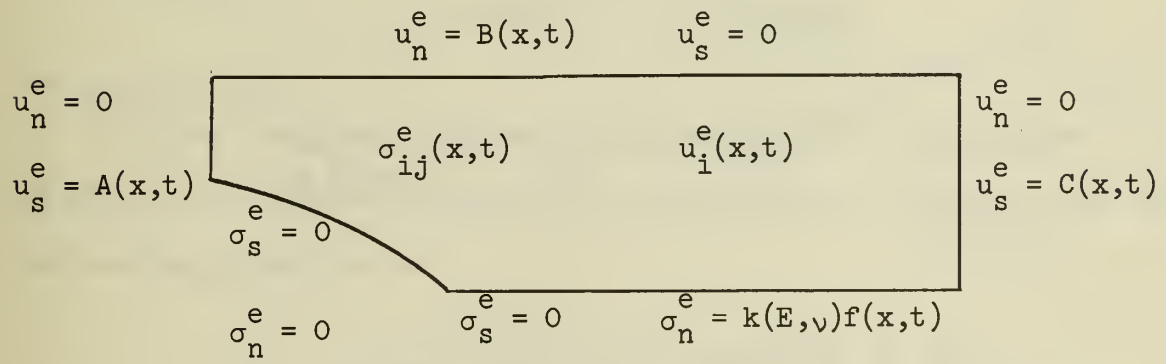

Fig. 6 Equivalent elastic problem.

The transform of this problem, which can now be computed because the boundary conditions of the moving crack are known for all time, is shown in Fig. 7.

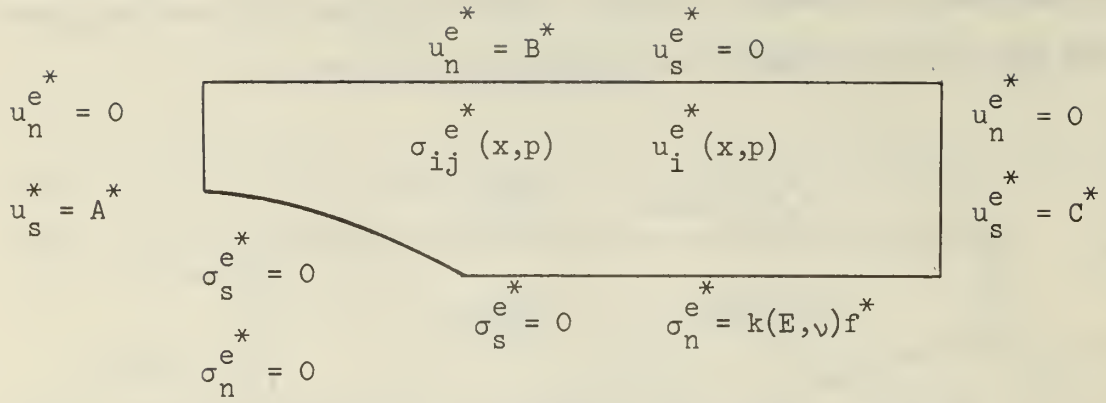

Fig. 7 Transform of equivalent elastic problem.

Now we define an equivalent viscoelastic problem whose boundary conditions are defined in a manner to "correspond" with Fig. 7. This is shown in Fig. 8.

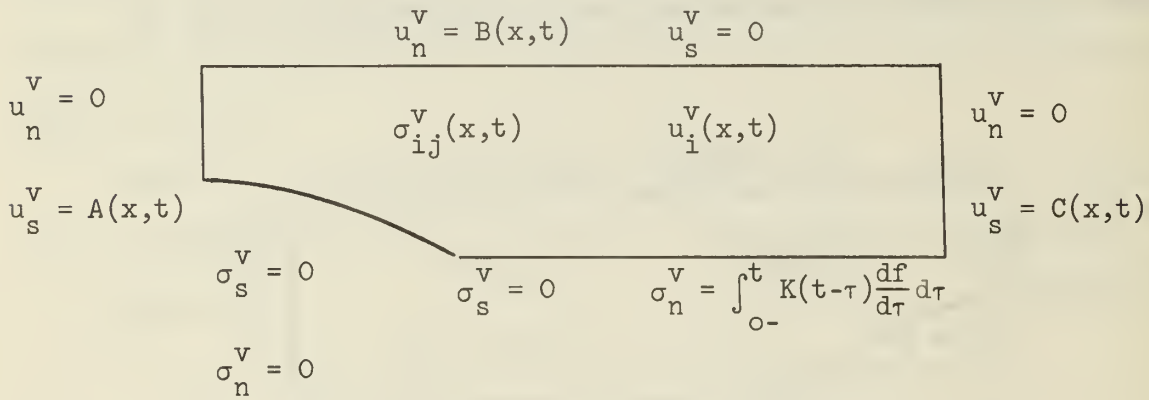

Fig. 8 Equivalent viscoelastic problem.

In Fig. 8, K(t) is defined as

$$K(t) = L^{-1}\left[\frac{k}{p}(E^*,\upsilon^*)\right] \tag{17}$$

The transform of this problem can also be computed by virtue of the definition of boundary values for all time. The results are shown in Fig. 9.

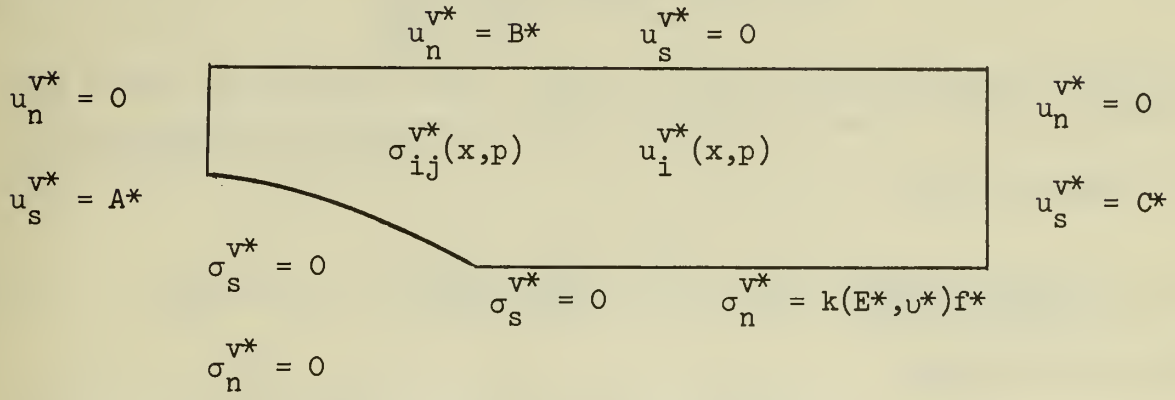

Fig. 9 Transform of equivalent viscoelastic problem.

Comparing the governing equations and boundary conditions for the problems shown in Fig. 7 and Fig. 9, it is seen that a correspondence exists.

$$\sigma_{ij}^{v*}(x,p) = \left[\sigma_{ij}^{e*}\right]_{\substack{E \to E^* \\ \upsilon \to \upsilon^*}} \tag{18}$$

This will also be a correspondence principle for the original problem of Fig. 4 if it can be shown that on the extension in front of the crack the boundary condition of

$$\sigma_n^v = \int_{o-}^{t} K(t-\tau)\frac{df}{d\tau}\, d\tau \tag{19}$$

produces $u_n^v = 0$ over the same surface. It goes without saying that the zero shear stress condition must exist due to the assumed symmetry of loading and geometry.

Using the extended correspondence principle, the displacements on the boundary are

$$u_n^{v*}(x,p) = \left[u_n^{e*}(x,p) \right]_{\substack{E \to E^* \\ \upsilon \to \upsilon^*}} \tag{20}$$

by symmetry $u_n^e = 0$, and $u_n^{e*} = 0$. If there are no material constants in u_n^{e*}, then from (20),

$$u_n^{v*} = u_n^{e*} \tag{21}$$

and on the boundary

$$u_n^{v} = u_n^{e} = 0 \tag{22}$$

Thus, the problem shown in Fig. 8 is the same as the original one in Fig. 4 for which a solution is being sought, and a correspondence principle has been established for this case.

Applying Equation (18) to the elastic stress solution of the long strip with displacement boundary conditions, we obtain

$$\sigma_{ij}^{v*} = \left\{ \sqrt{\frac{4}{3b\pi}} E \left[\frac{v_o(t)\, f_{ij}[\theta(t)]}{\sqrt{2(x - c(t))}} \right]^* \right\}_{E \to E^*} \tag{23}$$

Inverting the transform,

$$\sigma_{ij}^{v} = \sqrt{\frac{4}{3b\pi}} \int_{o-}^{t} E_{REL}(t-\tau)\, \frac{d}{d\tau} \left[\frac{v_o(\tau) f_{ij}[\theta(\tau)]}{2\sqrt{x - c(\tau)}} \right] d\tau \tag{24}$$

where

$$E^* = S\, E_{REL}{}^*$$

If we look at a point on the line of propagation,

$$\theta(t) = \pi\, h(t - t_1) \tag{25}$$

where t_1 is the time of arrival of the crack at the point of interest. Using Equation (25), it can be shown that f_{yy} in Equation (24) reduces to

$$f_{yy}\left[\theta(t)\right] = h(t) - h(t - t_1) \tag{26}$$

For a step displacement input, $v_o(t) = V_o h(t)$, the expression for opening mode stress simplifies to,

$$\sigma^v_{yy}(x,o,t) = V_o \sqrt{\frac{4}{3b\pi}} \int_{o-}^{t} E_{REL}\ (t - \tau)\ \frac{d}{d\tau}\left[\ \frac{h(\tau) - h(\tau - t)}{\sqrt{2\,(x - c(\tau))}}\right] d\tau \tag{27}$$

Carrying out the differentiation, and simplifying

$$\sigma^v_{yy}(x,o,t) = V_o \sqrt{\frac{4}{3b\pi}}\left[\frac{E_{REL}(t)}{\sqrt{2(x - c_o)}} + \int_o^{t_1} \frac{E_{REL}(t - \tau)\ c(\tau)}{[2(x - c(\tau)]3/2}\ d\tau\ \right] \tag{28}$$

With this expression for hoop stress, the stress intensity factor can be obtained via the definition of Equation (5).

$$K^v_1(t) = \lim_{x \to c(t)} \sqrt{2(x - c(t)}\ \ V_o \sqrt{\frac{4}{3b\pi}}\left[\frac{E_{REL}(t)}{\sqrt{2(x - c(t)}} + \int_o^{t_1} \frac{E_{REL}(t - \tau)\dot{c}(\tau)}{[2(x - c(t))]^3/2} d\tau\right] \tag{29}$$

It goes without saying that this equation is difficult to use in data reduction for crack propagation tests. This has led to a search for an approximate solution possessing a simpler, more usable form.

APPROXIMATE VISCOELASTIC STRESS DISTRIBUTION

The expressions for the elastic stress distribution in the neighborhood of a crack tip can be written as

$$\sigma^e_{ijs} = \frac{K^e_{is}\ (E,\sigma,c)}{\sqrt{2\,r}}\ f_{ij}(\theta) \tag{30}$$

where superscript e denotes elastic and subscript s denotes stationary crack. The functional dependence of K upon E,σ, and c, indicates that the stress intensity factor is in general a function of material, loading and crack length. Because the crack is stationary, the viscoelastic correspondence principle is applicable.

$$\sigma_{ijs}^{v*} = \frac{K_{is}^{e*}(E^*,\sigma^*,c)}{\sqrt{2\,r}}\, f_{ij}(\theta) \tag{31}$$

Inverting the transform,

$$\sigma_{ijs}^{v} = \frac{K_{is}^{e}}{\sqrt{2r}}\,(E(t),\sigma(t),c)\, f_{ij}(\theta) \tag{32}$$

where as before, to fit the definition,

$$K_{is}^{v} = L^{-1}\left[K_{is}^{e*}(E^*,\sigma^*,c)\right] \tag{33}$$

For slowly moving cracks, the inertia terms in the equilibrium equations can be neglected, and the field equations for the moving crack become identical to those for the stationary crack. If it were not for the changing boundary conditions at the crack tip, the two solutions would be identical; however the S.I.F. is altered as the crack propagates because the geometry of the body is changing and

$$K_{1s}^{v} \neq K_{1}^{v} \tag{34}$$

In the case of the long strip laboratory sample, the specimen approximates on infinite strip containing a semi-infinite crack. As the crack propagates, the geometry remains unchanged to the degree that the specimen models the infinite sheet; in fact, any geometry for which the crack propagation makes minor perturbations on the nature of the body, such as infinite domains, will be well represented by

$$K_1^v(t) = [K_{is}^v]_{c \to c(t)} \tag{35}$$

To illustrate this, consider an infinite sheet with a central crack of length 2c.

$$K_{is}^e = \sigma\sqrt{c} \tag{36}$$

By the correspondence principle and the definition of Equation (33),

$$K_{is}^v = L^{-1}\left[\sigma^*\sqrt{c}\right] = \sigma(t)\sqrt{c} \tag{37}$$

Using the approximation of Equation (35), the viscoelastic S.I.F. for a moving crack is found to be

$$K_1^v = \sigma(t)\sqrt{c(t)} \tag{38}$$

In this case, this is exactly the expression that results from the more rigorous extended correspondence principle.

Infinite Strip With Displacement Boundary Conditions

Beginning with the elastic solution for a stationary crack in a long strip,

$$\sigma_{ijs}^e = \sqrt{\frac{4}{3b\pi}} E\left[\frac{v_o(t)}{\sqrt{2(x-c)}}\right] F_{ij}(\theta) \tag{39}$$

By the classical correspondence principle,

$$\sigma_{ijs}^{v*} = \sqrt{\frac{4}{3b\pi}} E^*\left[\frac{v_o^*}{\sqrt{2(x-c)}}\right] F_{ij}(\theta) \tag{40}$$

Inverting the transform, still holding the crack stationary,

$$\sigma_{ijs}^v = \sqrt{\frac{4}{3b\pi}} \frac{F_{ij}(\theta)}{\sqrt{2(x-c)}} \int_{o-}^{t} E_{REL}(t-\tau) \frac{dv_o}{d\tau} d\tau \tag{41}$$

For a step displacement loading,

$$v_o = V_o h(t)$$

$$\sigma_{ijs}^{v} = \sqrt{\frac{4}{3b\pi}} \frac{F_{ij}(\theta)}{\sqrt{2(x - c)}} V_o E_{REL}(t) \tag{42}$$

Converting to a moving crack through the approximate relation of Equation (35), $\theta(t)$ is defined as before,

$$\sigma_{ij}^{v} = \sqrt{\frac{4}{3b\pi}} V_o \frac{E_{REL}(t)}{\sqrt{2(x - c(t)}} [h(t) - h(t - t_1)] \tag{43}$$

The stress intensity factor is readily recognizable from this form as

$$K_1^{v}(t) = \sqrt{\frac{4}{3b\pi}} V_o E_{REL}(t) \tag{44}$$

In order to measure this quantity on each specimen directly which would account for any specimen to specimen variation in $E_{REL}(t)$, we seek to express the S.I.F. in terms of stress. For a long strip without a crack, the principal elastic stress is

$$\sigma_y^{e} = \frac{E}{(1 - \upsilon^2)} \frac{V_o}{b} \tag{45}$$

Applying the correspondence principle to an incompressible strip,

$$\sigma_y^{v*} = \frac{4}{3b} E^* V_o^* \tag{46}$$

Upon inversion,

$$\sigma_y^{v}(t) = \frac{4}{3b} \int_{o-}^{t} E_{REL}(t - \tau) \frac{dv_o}{d\tau} d\tau \tag{47}$$

For a step strain history, $v_o = V_o h(t)$

$$\sigma_y^v(t) = \frac{4}{3b} V_o E_{REL}(t) \tag{48}$$

From Equation (44),

$$K_1^v(t) = \sqrt{\frac{3b}{4\pi}} \sigma_y^v(t) \tag{49}$$

By using the stress expression for an uncracked strip, $\sigma_y^v(t)$ represents the stress in the undisturbed field far out in front of the crack. In order to reduce laboratory data, it is necessary to relate the total load on the specimen, or the displacement of the specimen grips, to the far field stress. This has been accomplished through a finite element program.

Because the stress, $\sigma_y^v(t)$, is constantly relaxing during the test, the stress intensity factor is likewise decreasing. This results in the crack velocity steadily diminishing and approaching zero quite rapidly. The constantly varying crack velocity and, more particularly, the fact that it is approaching zero makes this test somewhat unattractive; however it is not impossible to use.

Infinite Strip with Stress Boundary Conditions

The same method when applied to the infinite strip with stress boundary conditions leads to considerably different results. Beginning with the elastic solution, (11)

$$K_1^e = \sigma \sqrt{\frac{b}{\pi}} \tag{50}$$

The viscoelastic stress intensity factor for a stationary crack can be obtained from Equation (33)

$$K_{is}^v = \sigma(t) \sqrt{\frac{b}{\pi}} \tag{51}$$

Since the stress intensity factor is independent of crack length, it is the same for a slowly moving crack as for a stationary one.

$$K_1^v(t) = \sigma(t)\sqrt{\frac{b}{\pi}} \tag{52}$$

This agrees exactly with the rigorous solution obtained in Equation (16). Thus if stress is held constant, the stress intensity factor remains constant and so does the velocity. However, this test is very difficult to run in actual practice. Because the specimen is not actually infinite, the net cross-section stress is difficult to hold constant as the crack runs.

Hertzler[13] has painstakingly done this in order to obtain data for this particular loading condition; however it is much more convenient to work with constant load.

Infinite Strip With Constant Load Boundary Conditions

Probably the most convenient approach to viscoelastic fracture characterization from the experimental point of view is to apply a constant load. A strip specimen is bonded between rigid grips as in the case of displacement boundary conditions. (See Figure 10.)

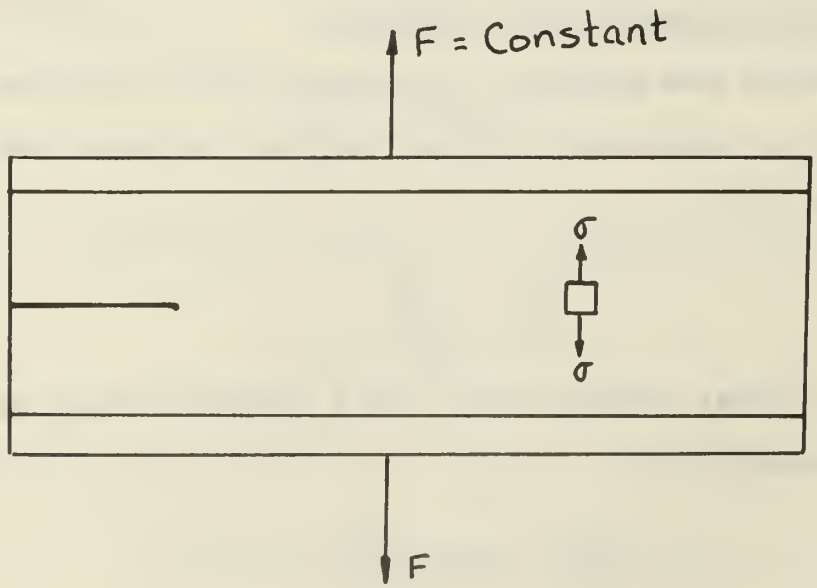

Fig 10. Constant Force Sheet

The S.I.F. for this specimen in terms of the far-field stress is given in equation (49).

$$K_1^V(t) = \sigma(t) \sqrt{\frac{3b}{4\pi}} \tag{53}$$

The relationship between $\sigma(t)$ and the applied force has been obtained from a finite element solution for a 1" x 6" specimen which has been used in this research program. For crack lengths up to three inches, the difference between the far-field stress in the undisturbed region and the average stress based on net cross-section was less than 1%. Considering this error to be negligible,

$$K_1^V(t) = \frac{F(t)}{A(t)} \sqrt{\frac{3b}{4\pi}} \tag{54}$$

where $F(t)$ is the applied force and $A(t)$ is the net cross-sectional area computed from the specimen length minus the crack length.

The variation of A with crack length will be very slight when the crack is small compared to the sheet length, which should be the domain of most, if not all, of the test. By varying the level of applied force, the velocity of crack propagation in the sheet is varied. For a given force, the S.I.F.

is virtually constant as mentioned before; consequently the velocity of crack propagation will also be constant. A plot of K_1^v vs. $\dot{c}(t)$ completes the characterization.

Infinite Strip--Constant Displacement Rate

A good test case to which the fracture characterization might be applied is the infinite strip subjected to a constant displacement rate loading. Having obtained the fracture characterization of K_1^v vs. $\dot{c}$ via the constant load test, it is possible to predict the crack behavior for the same strip under constant displacement rate and check the results experimentally.

From the elastic solution,

$$K_1^e = \sqrt{\frac{4}{3b\pi}}\, E\, v_o \tag{55}$$

Using the correspondence relation of Equation (33),

$$K_1^{v*} = \sqrt{\frac{4}{3b\pi}} E^* v_o^* \tag{56}$$

Inverting the transform,

$$K_1^v(t) = \sqrt{\frac{4}{3b\pi}} \int_{o-}^{t} E_{REL}(t-\tau)\, \frac{dv_o}{d\tau}\, d\tau \tag{57}$$

For constant displacement rate, R,

$$K_1^v(t) = \sqrt{\frac{4}{3b\pi}} R \int_{o-}^{t} E_{REL}(t-\tau) d\tau \tag{58}$$

The integral can be evaluated by means of a Prony Series representation of the relaxation modulus.

$$E_{REL}(t) = \Sigma\, E_i e^{-\alpha_i t} + E_r \tag{59}$$

Substituting into the above

$$K_1^v(t) = \sqrt{\frac{4}{3b\pi}} R \left\{ \Sigma \left[\frac{E_i}{\alpha_i} \left(1 - e^{-\alpha_i t} \right) \right] + E_r t \right\} \qquad (60)$$

From this expression and the fracture characterization, a crack history can be predicted. This solution is applicable for crack lengths that approximate the infinite strip condition. Once the crack becomes great enough, by comparison to the length of the strip, to cause the far-field stress to deviate from the net section stress when it runs, the above expression will begin to be in error. The amount of the error can be determined numerically.

FRACTURE CHARACTERIZATION

The first two methods of fracture characterization previously discussed have been carried out experimentally by C. M. Hertzler[13]. The others will be carried out in the near future.

Constant Displacement Case

Tests were conducted on cracked biaxial strip specimens with displacement boundary conditions. The strips were six inches in length, one inch in width (2b) and 1/10 inch thick. Redwood tabs bonded to the horizontal edges allowed for gripping. An initial crack of 0.75 inch was cut, as suggested by Mueller[9], and the length of the propagating crack was measured as a function of time with an optical comparator.

The testing was performed with the apparatus, which consisted of an Instron Universal Testing Machine equipped with special jaws to clamp the specimen and apply displacement v_o while maintaining the upper and lower boundaries parallel. The displacement was applied at rates ranging from one inch/minute for low temperatures to five inches/minute at the high temperatures. A conditioning chamber allowed the tests to be conducted at the same specific temperatures as in the previous case. After waiting ten times the loading time the ramp tests simulated step displacement loading, $v_o h(t)$, for

which the stress intensity factor reduces to Equation (44). As time proceeds after loading, the stress intensity factor is monotonically decreasing as a result of relaxation. This produces a corresponding decrease in crack velocity, which was observed experimentally.

The stress intensity factor for each test was calculated by using Equation (49) and plotted on a graph of stress intensity factor versus crack velocity for each specific testing temperature (see Figs. 11 through 16). A conventional a_T shift was attempted with the data, and a smooth master curve was obtained graphically by shifting the curves for various temperatures along the abscissa, relative to the curve at T_o to produce a continuous function. The resulting characterization curve is shown in Fig. 17 where $T_o = 70^oF$, and $a_T = 1$. It turned out that the a_T curve for the fracture characterization corresponded exactly with the a_T curve for modulus.

Constant Stress

The specimen configuration used to achieve the stress boundary conditions is shown in Fig. 18. The specimen was cut from samples designed for use in biaxial tests with a gage length of 1.0 inch and thickness of 0.1 inch. The wooden tabs were segmented with saw cuts, which stopped in the adhesive bond just short of the propellant. (To penetrate through the bond into the propellant would have created a stress riser and a point of probable crack initiation.) The width, w, ideally would be very small, allowing shear-free edges; however, practical considerations forced a width of w = 0.25 inch.

Initial experiments, with the right-hand edge of the propellant flush with the wooden tab edge, showed that soon after loading a fast running crack would initiate at a local defect along the right edge of even a carefully cut specimen. Adding a 1/8 inch unloaded length reduced the stress along this edge and eliminated the problem. To compensate for this departure from

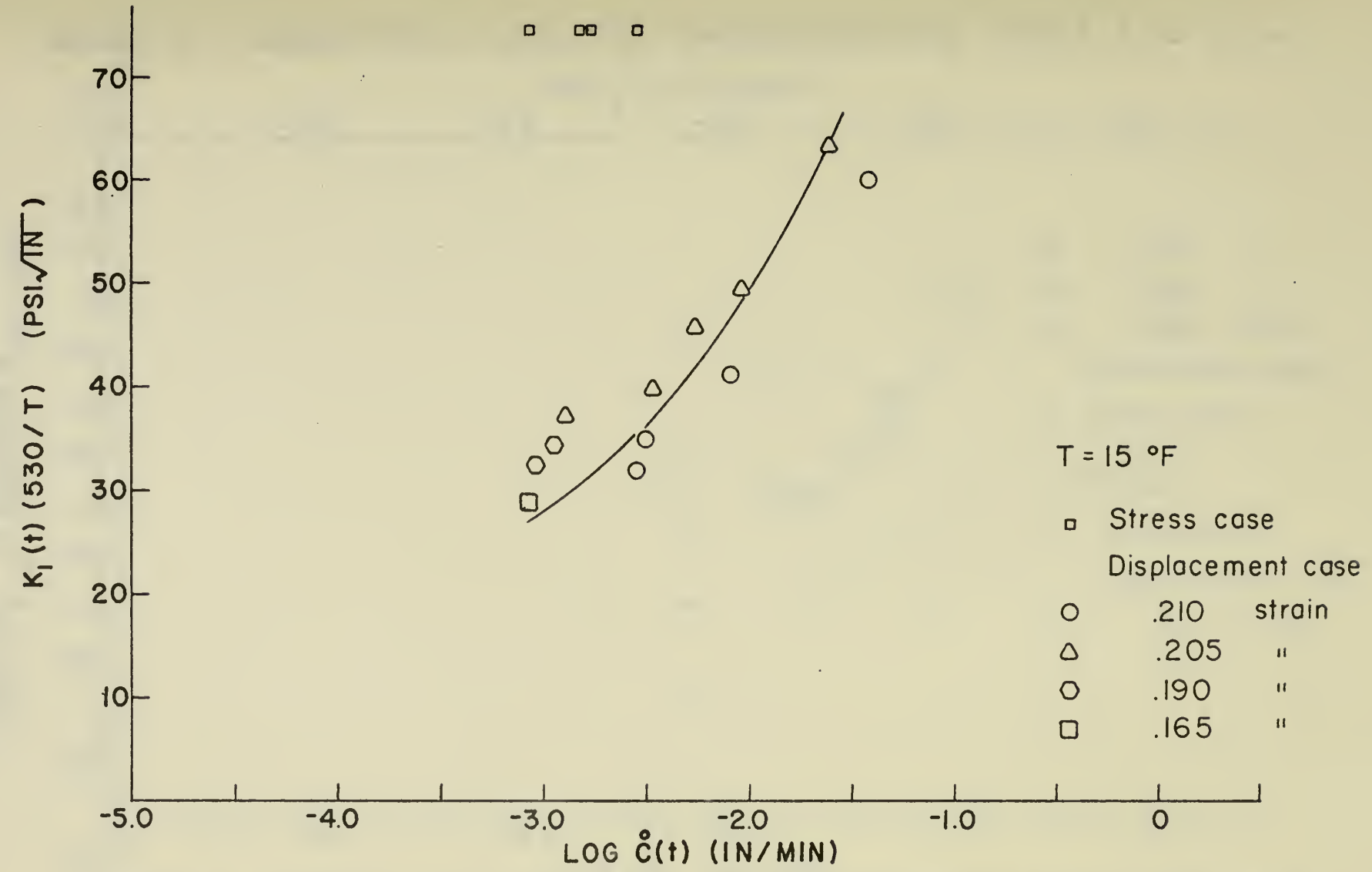

FIGURE 11 PROPELLANT FRACTURE CHARACTERIZATION CURVE FOR 15 °F

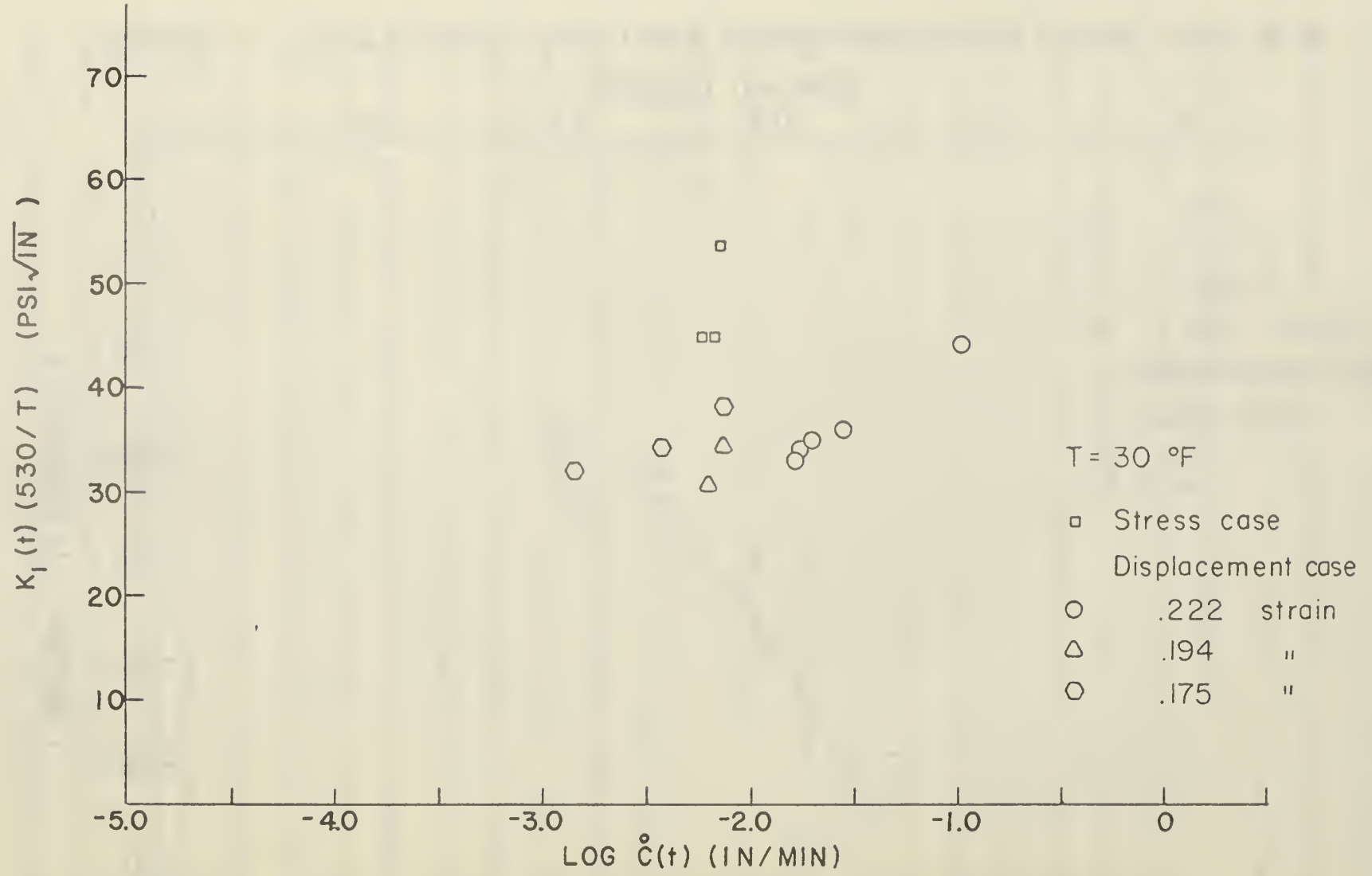

FIGURE 12 PROPELLANT FRACTURE CHARACTERIZATION CURVE FOR 30 °F

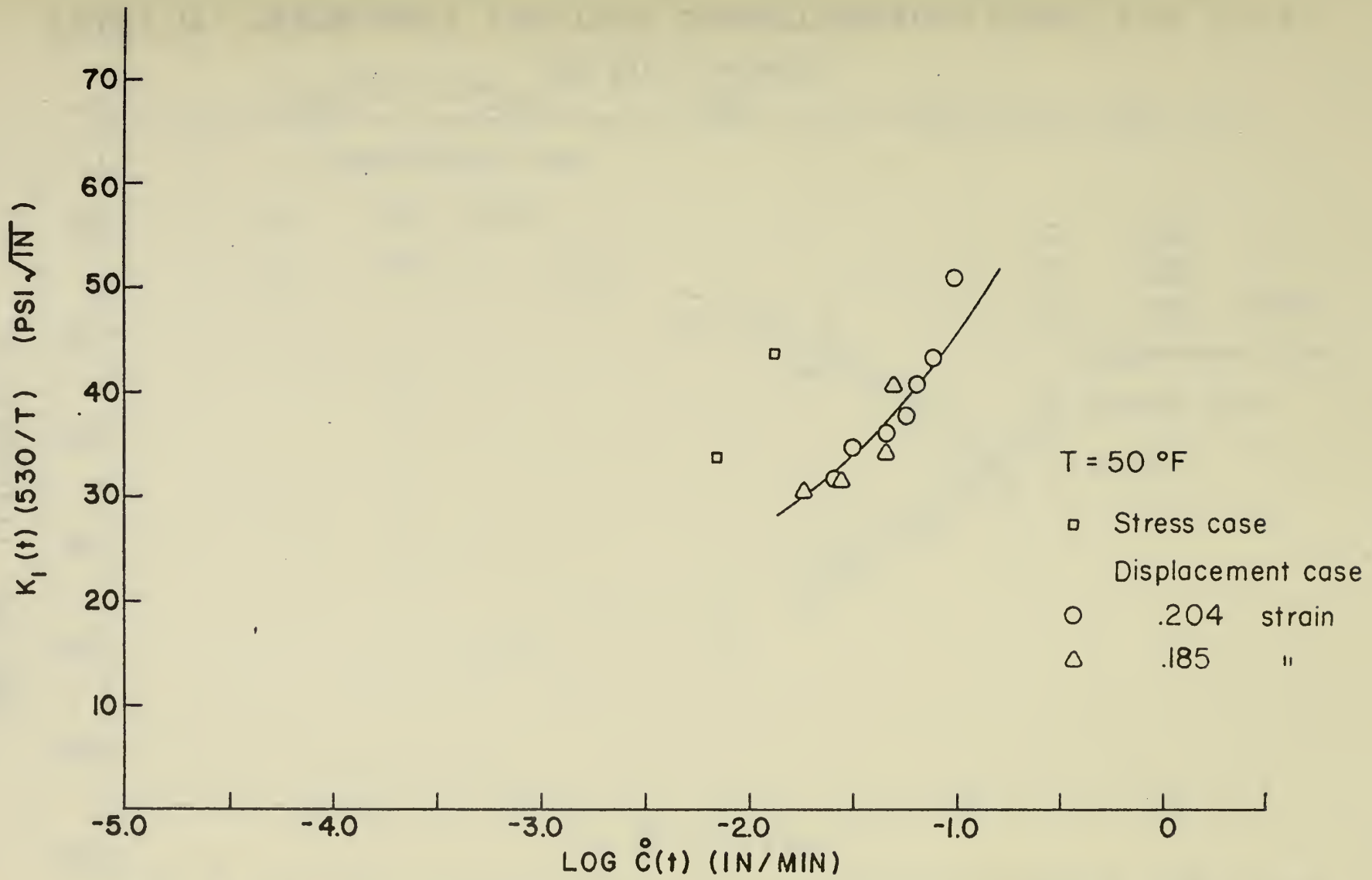

FIGURE 13 PROPELLANT FRACTURE CHARACTERIZATION CURVE FOR 50 °F

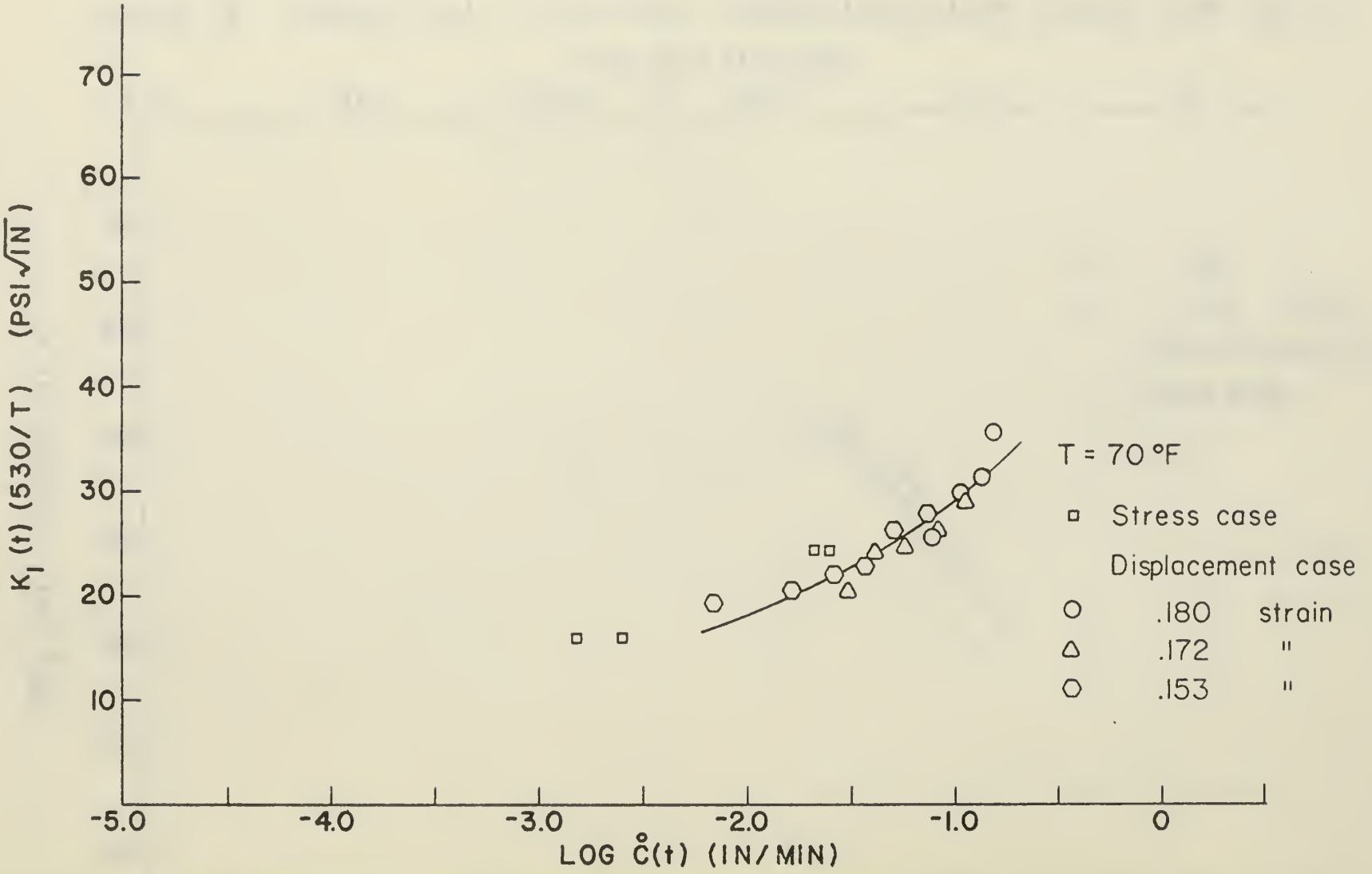

FIGURE 14 PROPELLANT FRACTURE CHARACTERIZATION CURVE FOR 70 °F

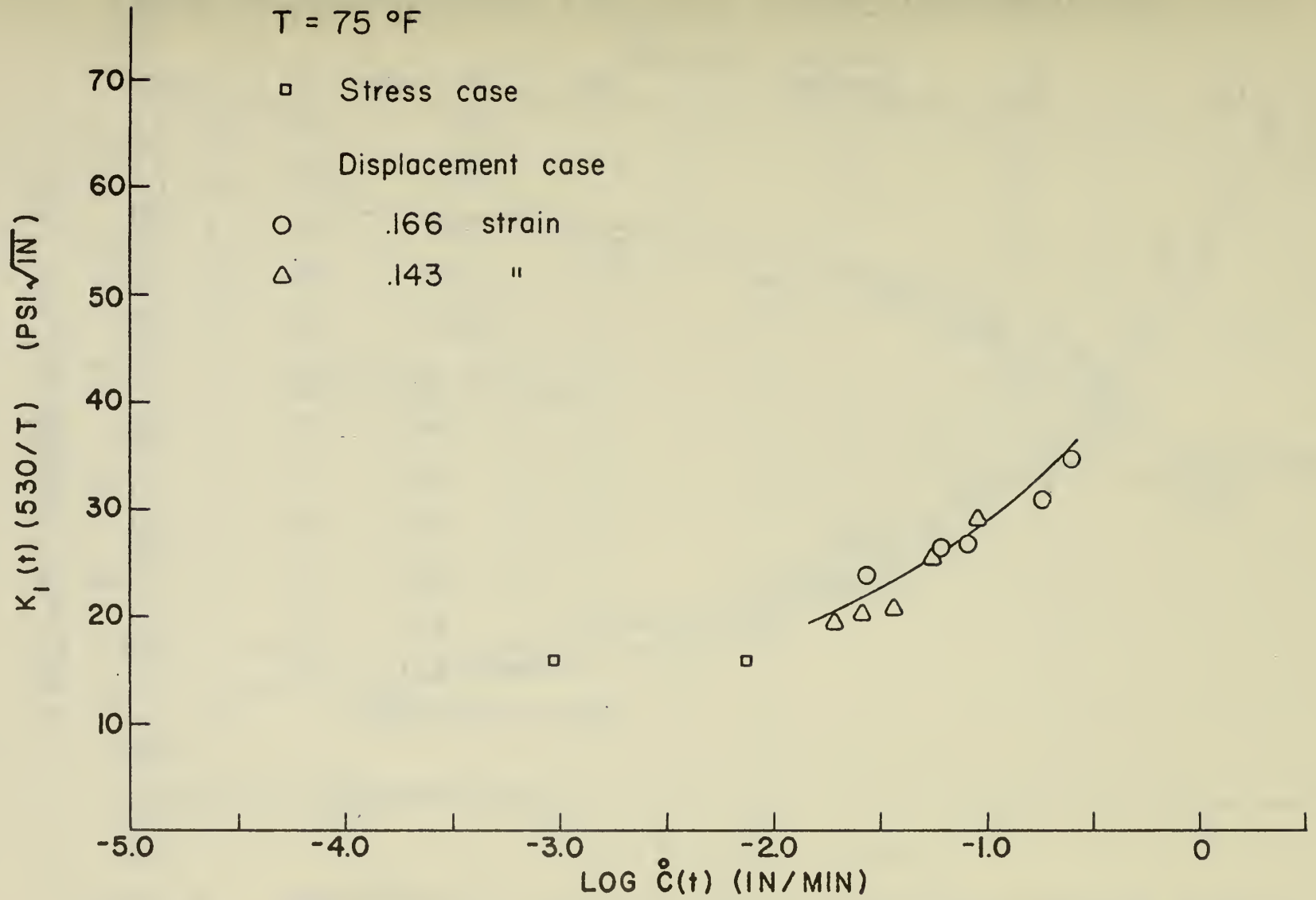

FIGURE 15 PROPELLANT FRACTURE CHARACTERIZATION CURVE FOR 75 °F

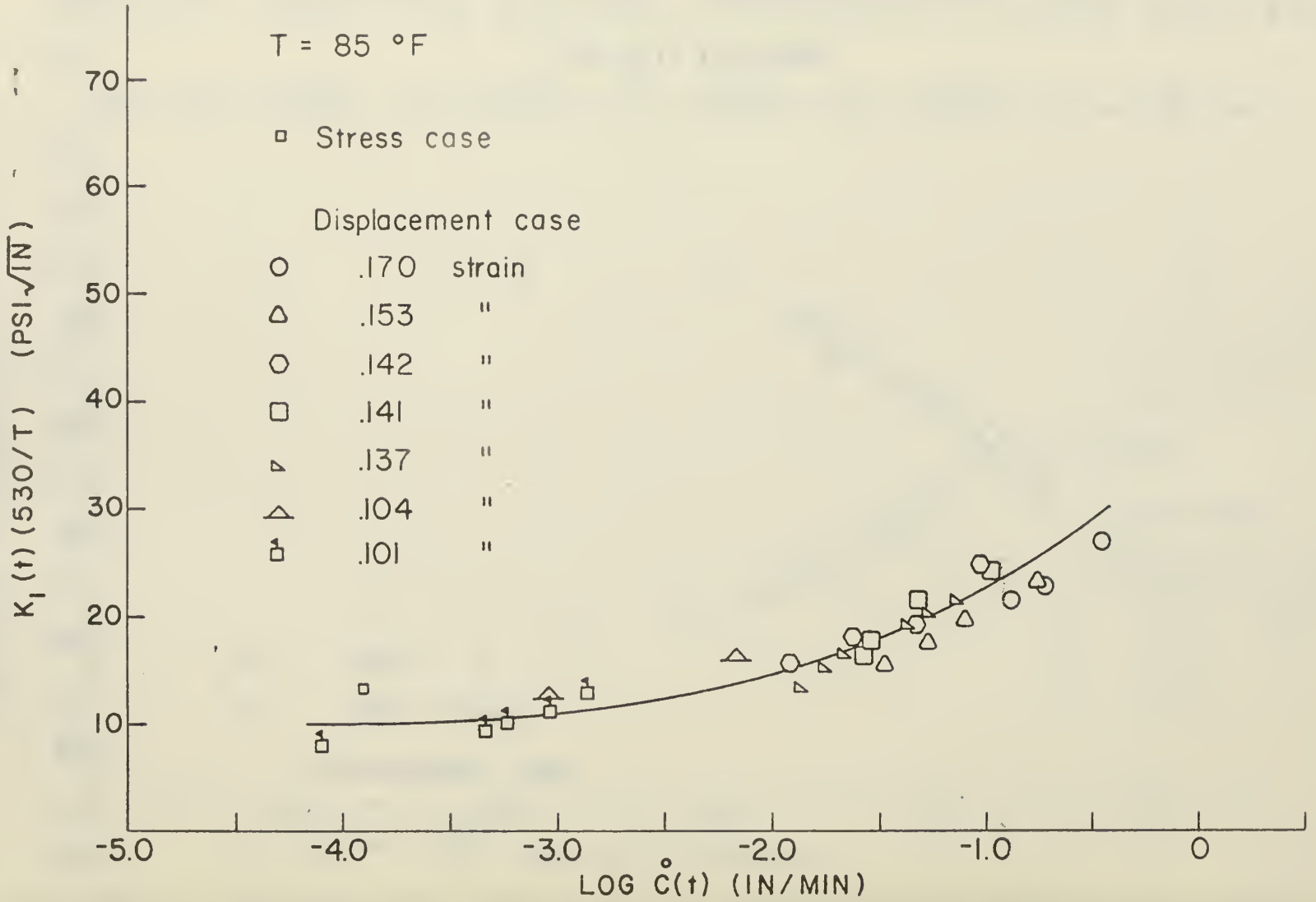

FIGURE 16 PROPELLANT FRACTURE CHARACTERIZATION CURVE FOR 85 °F

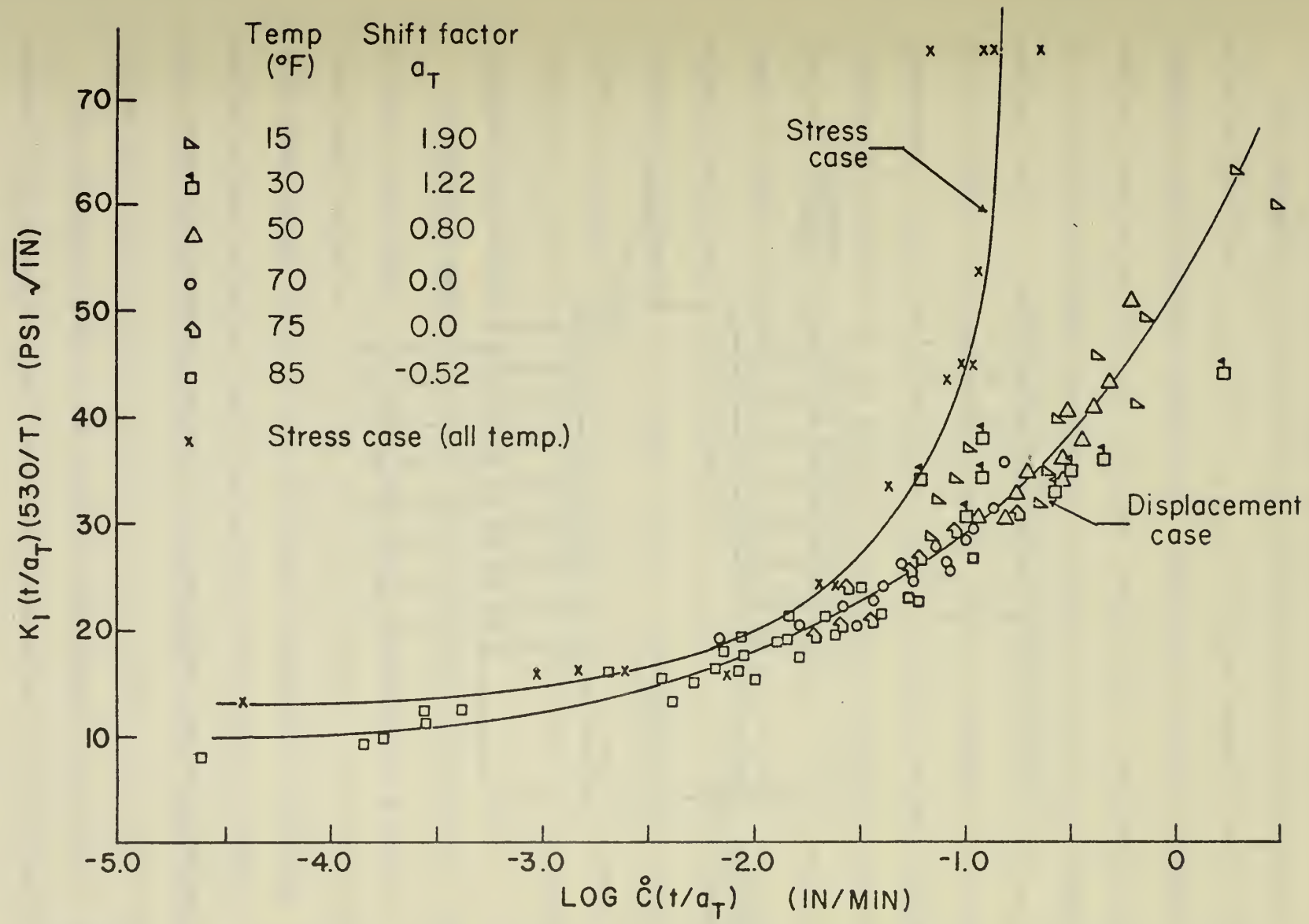

FIGURE 17 PROPELLANT FRACTURE CHARACTERIZATION MASTER CURVE

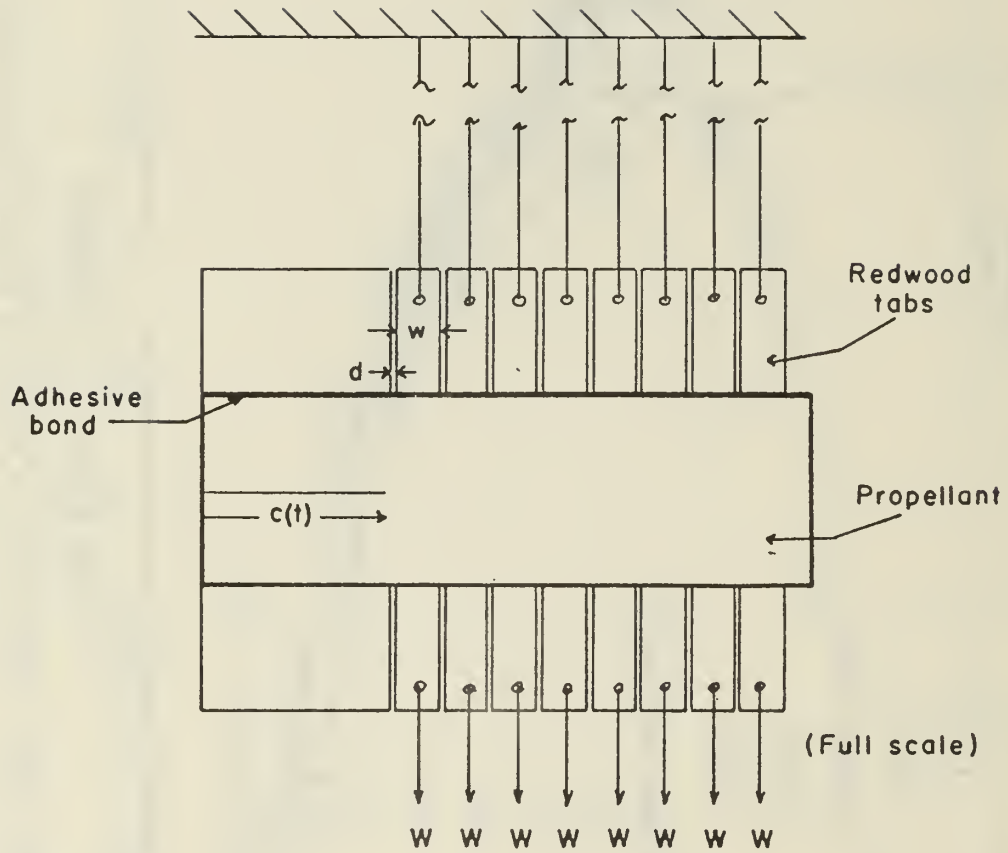

Fig. 18 Specimen configuration for stress boundary conditions.

uniform stress at the right hand edge and yet still meet the restriction leading to Equation (52), $c(t)_{max}$ was limited to 2.0 inches.

The thickness of the saw cuts in the wooden tabs was large enough to allow unrestrained ϵ_x, or $d/w \geq \epsilon_{x\ max}$. The upper segments were individually suspended and the lower segments were individually loaded by weights W. An initial crack of one inch was cut with a razor blade. Horizontal extension of the crack and constant propagation velocity were taken as evidence of uniform loading. Each specimen was tested by applying all loads at $t = 0$, and the length of the propagating crack, $c(t)$, was measured with an optical comparator. As the crack passed a segment, the weight on that segment was removed in proportion to the width of the segment traversed by the crack. The tests were conducted in an environmental chamber with the relative humidity less than 30%, at six temperatures ranging from 15°F to 85°F. The crack velocity was slower in this geometry for a given S.I.F. than it was under constant displacement as is shown in Figs. 11 through 16. The shifted master curve for constant stress, which is shown in Fig. 17, was obtained by using the same a_T shift factor as was determined in the first set of tests for constant displacement.

Differences in the fracture behavior of the load histories is thought to be due to dewetting. The theory developed considers only a purely viscoelastic material. However, the solid propellant was a filled material, which when loaded, exhibited the additional mechanism of dewetting. Wood[14] has shown that propellant dewetting is not a rate process, rather it occurs upon initial application of stress. This behavior has a significant bearing on the experimental results obtained in this study as will now be shown.

In both cases tested, the measured load parameter was stress, thus automatically accounting for the modulus relaxation in the displacement case. However, the two stress histories were quite different as shown in Fig. 19.

In the stress case, stress was constant while in the displacement case there was an initial extremely high stress which continually relaxed.

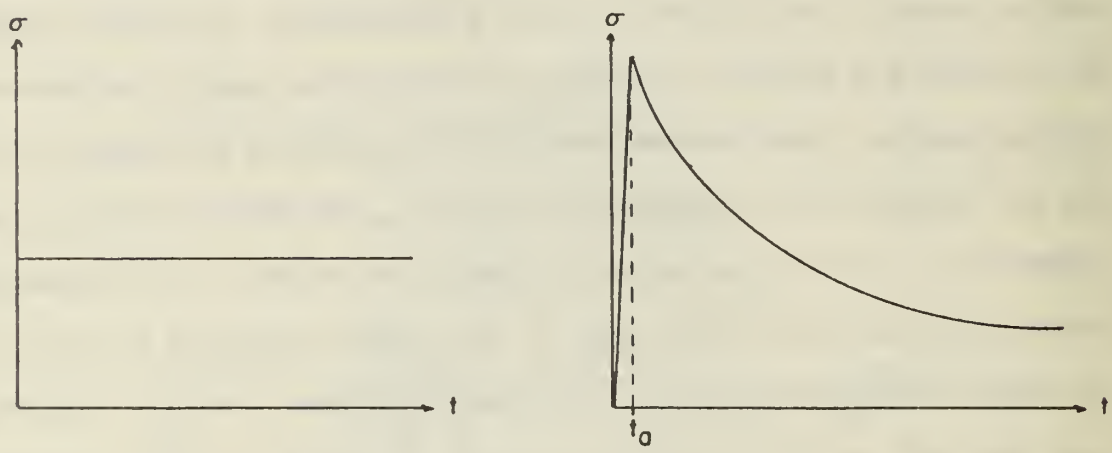

Constant Stress Constant Displacement

Fig. 19 Stress histories.

Thus a sample tested in the stress case exhibited minimum dewetting because of its history of constant stress. However, in the displacement case, for a corresponding stress at $t \geq 10t_a$ (where t_a is the time required to apply the load) much more dewetting had occurred due to the initial high stress. Consequently the crack propagated through a material which had been significantly altered from that in the stress case. The propagating crack had fewer bonds to break per unit area, compared with the stress case, and accordingly its velocity was as much as two orders of magnitude higher. This produced significantly different characterization curves for the two cases as shown in Fig. 17.

Since dewetting produces microscopic voids in the material, stiffness is reduced as dewetting increases. Using this fact, the increased dewetting of the displacement case was verified in preliminary tests at 15°F. In these tests, for identical stress and time, the modulus in the displacement case was one-half that of the stress case.

In an attempt to reduce the initial high stress peak in the displacement case, thus reducing the dewetting, additional preliminary tests at 15°F were conducted. The maximum stress was limited to that which produced stress intensity factors comparable with those of the stress case for the same temperature. Equivalent moduli showed that the amount of dewetting was in fact equivalent. However, as soon as the displacement rate was stopped, the stress relaxed due to $E_{REL}(t)$. Thus even if the crack propagated at the same velocity as in the stress case (approximately 0.1 inch per hour) relaxation of the driving stress decelerated the crack to zero velocity over distances too small to be accurately measured. Thus, no additional characterization data were obtainable with this loading method.

The accuracy of the measured velocity in the stress case was considered superior to that of the displacement case, especially for low velocities. For in the displacement case, c(t) had to be measured over relatively short periods of time to obtain an accurate crack propagation function. (Velocity was obtained by graphically measuring the slope of this function.) As c(t) became small, $\Delta c(t)$ for the time interval mentioned above also became small. Thus, because the experimental crack propagation was irregular due to inhomogeneities in the propellant, the actual velocity was obscured as those irregularities approached the magnitude of $\Delta c(t)$. However, in the stress case, $\dot{c}(t)$ was a constant and $\Delta c(t)$ could be measured over large time intervals.

The scatter in the characterization curves is due to the inaccuracies mentioned above for the displacement case and also to the inhomogeneous nature

of a highly filled viscoelastic material such as propellant. By comparison, similar characterization of solithane, an unfilled and relatively more homogeneous material, by Francis et. al.[9] showed significantly less scatter.*

Referring to the characterization curves, in both cases there appears to be a K_1 critical below which a crack will not propagate. Again for both cases, especially apparent in the stress case, there appears to be a maximum velocity of propagation; however these maximum velocities are somewhat misleading. Preliminary tests showed that at very high loads the failure was general and catastropic, initiated at voids and other stress risers throughout the specimen as well as at the crack tip. Clean crack propagation was possible at high loads for low temperature, but high loads at room temperature precipitated fracture throughout the specimen resembling disintegration.

---

*Solithane at room temperature has a relaxation time of less than one minute. Thus, though tested for the displacement case, essentially constant velocity crack propagation in these tests allowed the additional advantage of increased accuracy of the measured crack propagation function for reasons mentioned above.

The purpose of all of the preceding material relative to making a fracture characterization is to obtain the base information required to analyze a rocket motor. Rocket motor geometries are generally complex and finite element methods are required to generate solutions and stress intensity factors even for elastic fracture predictions. A method will now be presented which uses the elastic methods to generate the desired viscoelastic fracture results.

Viscoelastic fracture analyses of rocket motor geometries compounds the two complexities of time dependent stress analysis and fracture mechanics. The expense of the undertaking, as well as the difficulty of doing it rigorously, suggests that approximate methods of solution be pursued and developed.

Appendix I has been written to give motivation to an approximate method of stress analysis commonly referred to as quasi-viscoelastic. In this development, a circular cylinder is used as the motor geometry, and it is assumed that the method holds for all geometries. With a means available for obtaining the stress field, another approximate analysis procedure is now presented to determine fracture behavior.

For most, if not all, two-dimensional geometries with through-the-thickness cracks, the stress intensity factor has a common form.

$$K_1 = \lambda\sigma\sqrt{c} \tag{61}$$

where λ is a modifying factor containing information relative to geometry, and in a sense, reflects the departure of the geometry in question from the infinite sheet with a central crack where $\lambda = 1$. λ includes influences such as boundaries, stiffeners, dimensionality of the stress

field, etc. σ is the applied uniaxial stress, and when cast in this form it is seen that σ represents the stress that would exist in the body at the location of the crack if there were no crack present. In other words, σ is the stress acting across the line of the crack in a identical geometry but without a crack. For the rocket motor shown in Fig. 20,

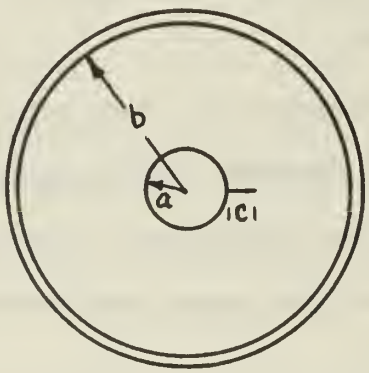

Fig. 20

the crack extends along the r direction, and the stress acting across the crack is σ_θ. The stress intensity factor for the motor can be written as

$$K_1 = \lambda \sigma_\theta \sqrt{c} \tag{62}$$

where the crack length is c, and the influence of the bore, case, transverse stress and material properties are included in λ. For a given configuration; the functional dependence of the quantities in Eq. (62) can be represented in terms of these parameters which will vary with time in a viscoelastic fracture analysis.

$$K_{1e} = \lambda(E,c)\ \sigma_\theta(E,p)\ \sqrt{c} \tag{63}$$

The subscript, e, designates elastic stress intensity factor, while E, c and p represent the modulus, crack length and pressure loading respectively. These are the quantities that will vary with time in a viscoelastic fracture analysis.

It is proposed that $\lambda(E,c)$ be found by numerical methods using finite element codes. Such a study was conducted by Francis[2], et. al. for elastic materials and they experimentally confirmed predictions made in this manner. For the geometry specified, the elastic stress intensity factor was computed from energy differences for runs with incrementally different crack lengths.

$$K_{1e}^2 = \frac{E \Delta U}{\pi t \Delta c} \tag{64}$$

(The procedure is defined in a note by Deverall and Lindsey[15].) Results are shown in Fig. 21 for a high modulus material. Similar curves could be constructed for the range of modulus values exhibited by propellant, and λ follows by dividing K_{1e} by σ_θ reevaluated at $r = a + c$.

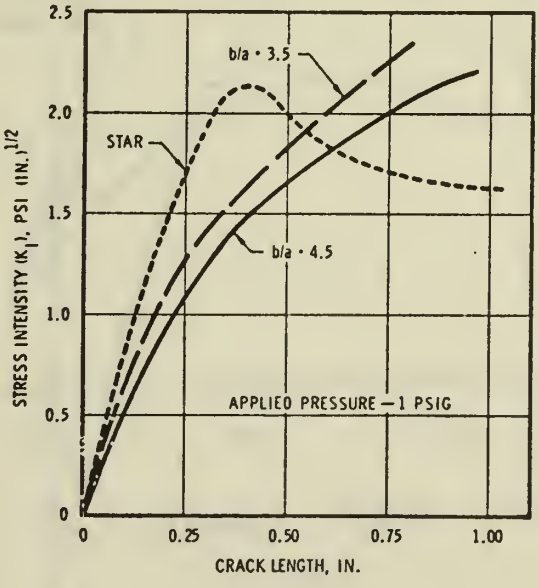

Fig. 21

Stress Intensity Factor vs. Crack Length

Two examples for low modulus materials were available from the literature in reference 2 for pressure loads. They are reproduced in Figs. 22a and 22b, and from them λ was computed to show the dependence of this factor on modulus. Of course this range of modulus is much greater than that found in rocket motors. However once these results are obtained λ is easily computed.

A plot of the results in Fig. 23 shows that λ is not strongly sensitive to changes in modulus. Two more runs in the range of modulus indicated by the dotted lines would provide the information needed to construct the viscoelastic solution that will now be developed in detail.

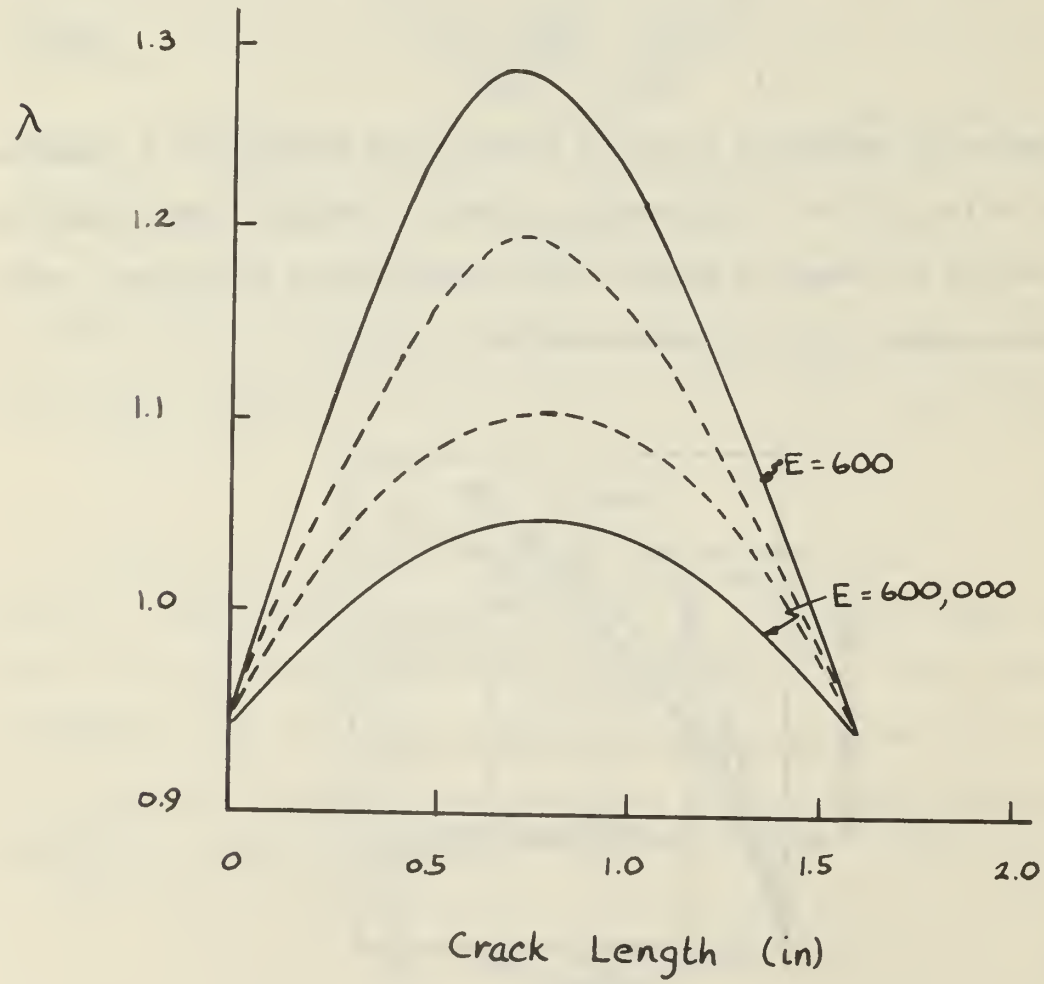

Fig. 23

λ vs. Crack Length

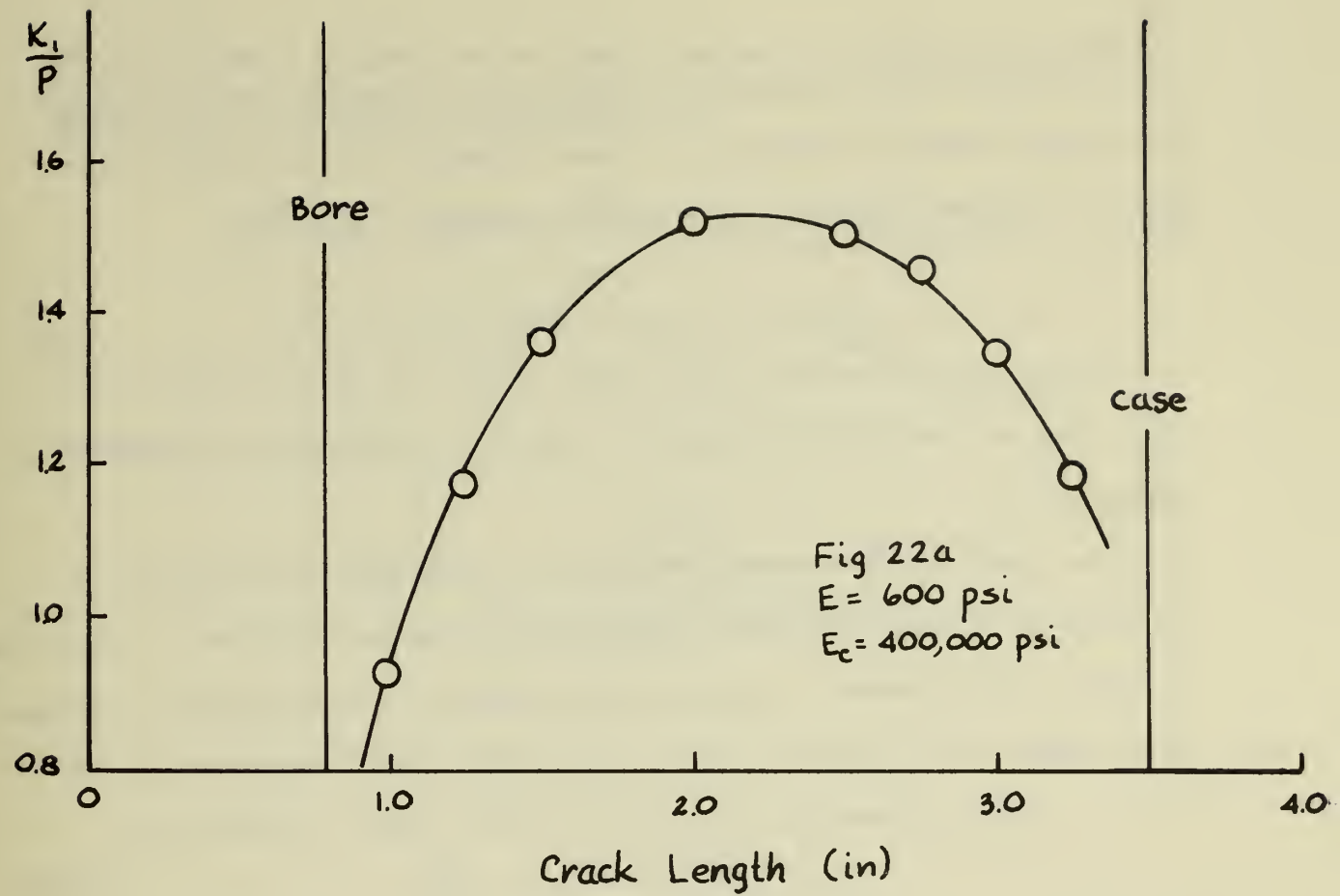
$\frac{K_1}{P}$
1.6
1.4
1.2
1.0
0.8
Bore
Case
0
1.0
2.0
3.0
4.0
Crack Length (in)
Fig 22a
E = 600 psi
E_c = 400,000 psi

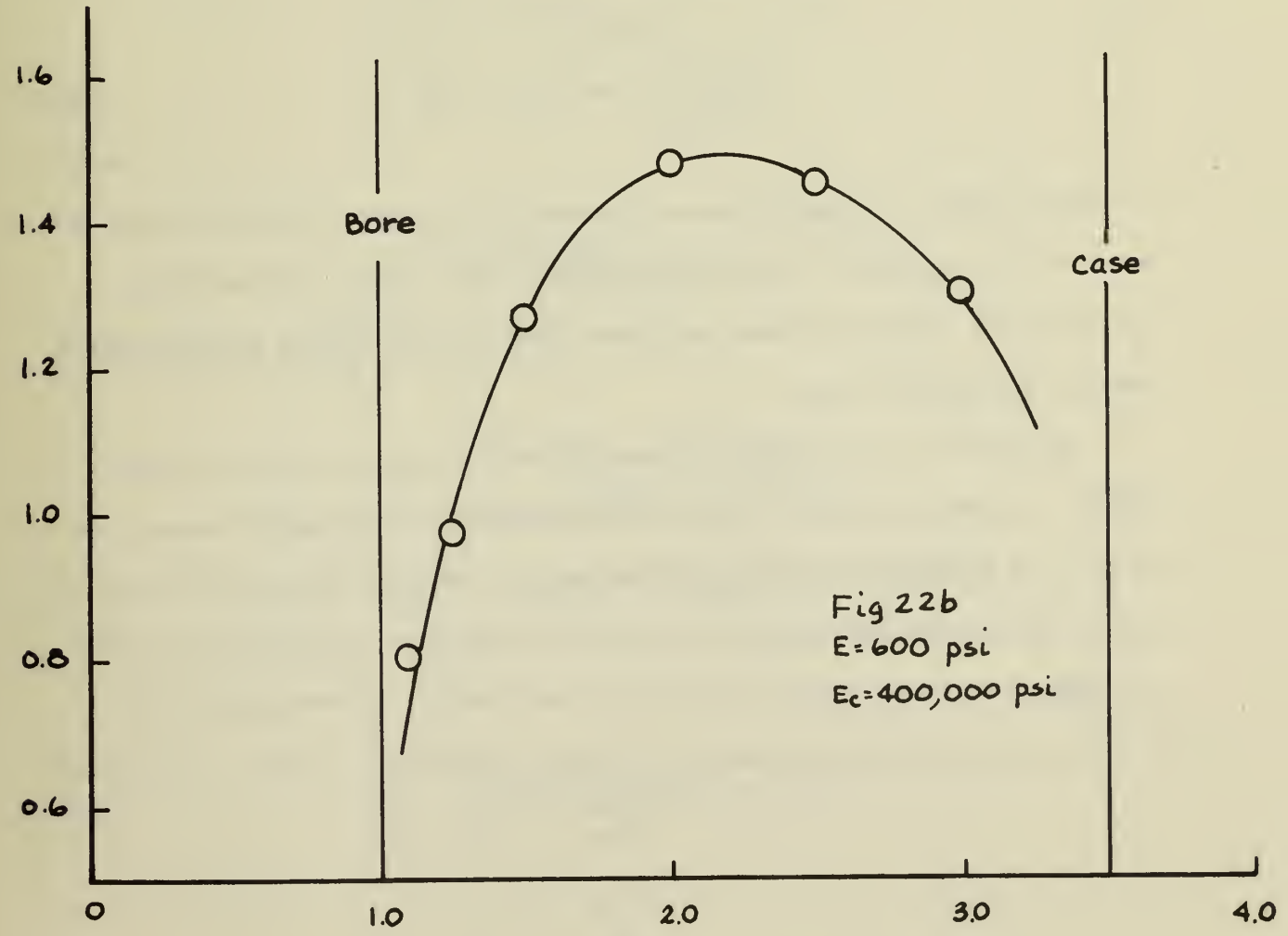
1.6
1.4
1.2
1.0
0.8
0.6
Bore
Case
0
1.0
2.0
3.0
4.0
Fig 22b
E=600 psi
E_c=400,000 psi

Consider first a stationary crack in this geometry. We have shown previously that the viscoelastic stress intensity factor for this case may be obtained from the correspondence principle (Eqn. 33).

$$K_{1s}^{v}(t) = L^{-1}\left[\lambda_{v}^{*}(E^{*},c)\ \sigma_{\theta}^{v*}(E^{*},p^{*})\ \sqrt{c}\ \right] \tag{65}$$

$\sigma_{\theta}^{v}(t)$ can be found from the elastic solution by the method outlined in Appendix I.

The viscoelastic correction factor, λ_{v}, can be found from Fig. 23 by using an equivalent elastic modulus, which can be found for the viscoelastic problem. To illustrate, the equivalent modulus for plane strain is defined as follows:

$$\epsilon_{\theta}^{v} = \frac{1+\upsilon}{E_{eq}}\left[(1-\upsilon)\ \sigma_{r}^{v} - \upsilon\sigma_{\theta}^{v}\right] \tag{66a}$$

$$\epsilon_{\theta}^{v} = \frac{1+\upsilon}{E_{eq}}\left[(1-\upsilon)\ \sigma_{\theta}^{v} - \upsilon\sigma_{r}^{v}\right] \tag{66b}$$

In other words, the instantaneous viscoelastic stress and strain can be used to find the value of Young's modulus which would produce those stresses and strains if the body were elastic. Of course the equivalent modulus varies with time.

The stresses and strains generally vary also from point to point within the motor; however for a cylinder the sum of normal stresses and strains is a constant throughout the motor. We will therefore choose to define the equivalent modulus in terms of this sum. Adding Eqns. (66a) and (66b),

$$\epsilon_{r}^{v} + \epsilon_{\theta}^{v} = \frac{(1+\upsilon)(1-2\upsilon)}{E_{eq}}\left[\sigma_{r}^{v} + \sigma_{\theta}^{v}\right] \tag{67}$$

The viscoelastic strains can be found in terms of viscoelastic stresses through the viscoelastic constitutive law.

$$\varepsilon_r^v + \varepsilon_\theta^v = (1+\upsilon)(1-2\upsilon) \int_{0-}^{t} D_{crp}\,(t-\tau)\,\frac{d}{d\tau}\,(\sigma_r^v + \sigma_\theta^v)d\tau \qquad (68)$$

Eliminating $(\varepsilon_r^v + \varepsilon_\theta^v)$ from Eqns. (67) and (68), the equivalent modulus becomes,

$$E_{eq}(t)\,\frac{\sigma_r^v + \sigma_\theta^v}{\int_{0-}^{t} D_{crp}\,(t-\tau)\frac{d}{d\tau}\,(\sigma_r^v + \sigma_\theta^v)d\tau} \qquad (69)$$

With this parameter determined, Fig. 23 can be used to find $\lambda_v(t) = \lambda[E_{eq}(t),c]$.

An inversion of Eqn. (65) for a fixed crack length yields

$$K_{ls}^v(t) = \sqrt{c} \int_{0-}^{t} \lambda_v(t-\tau)\,\sigma_\theta^v(\tau)d\tau \qquad (70)$$

where

$$\lambda_v(t-\tau) = [\lambda(E,c)]\;E = E_{eq}(t-\tau)$$

Referring back to Eqn. (69),

$$E_{eq}(t-\tau) = \frac{\sigma_r^v(t-\tau) + \sigma_\theta^v(t-\tau)}{\int_{0-}^{t-\tau} D_{crp}(t-\tau-\xi)\frac{d}{d\xi}\,[\sigma_r^v(\xi) + \sigma_\theta^v(\xi)]d\xi} \qquad (71)$$

With the geometry and material correction factor included in the analysis so that a continuous updating of these properties can be effected,

the correlation between static and dynamic viscoelastic stress intensity factor would follow from Eqn. (38).

$$K_I^V(t) = \sqrt{c(t)} \int_0^t [\lambda(E,c)]_{\substack{c=c(\tau) \\ E=E_{eq}(t-\tau)}} \sigma_\theta^V(\tau)d\tau \qquad (72)$$

Schematically the solution may be viewed to proceed as shown in Fig. 24. The static viscoelastic solution is given for a variety of crack lengths. The viscoelastic stress intensity factor for a moving crack is assembled from the incremental pieces of the static solution.

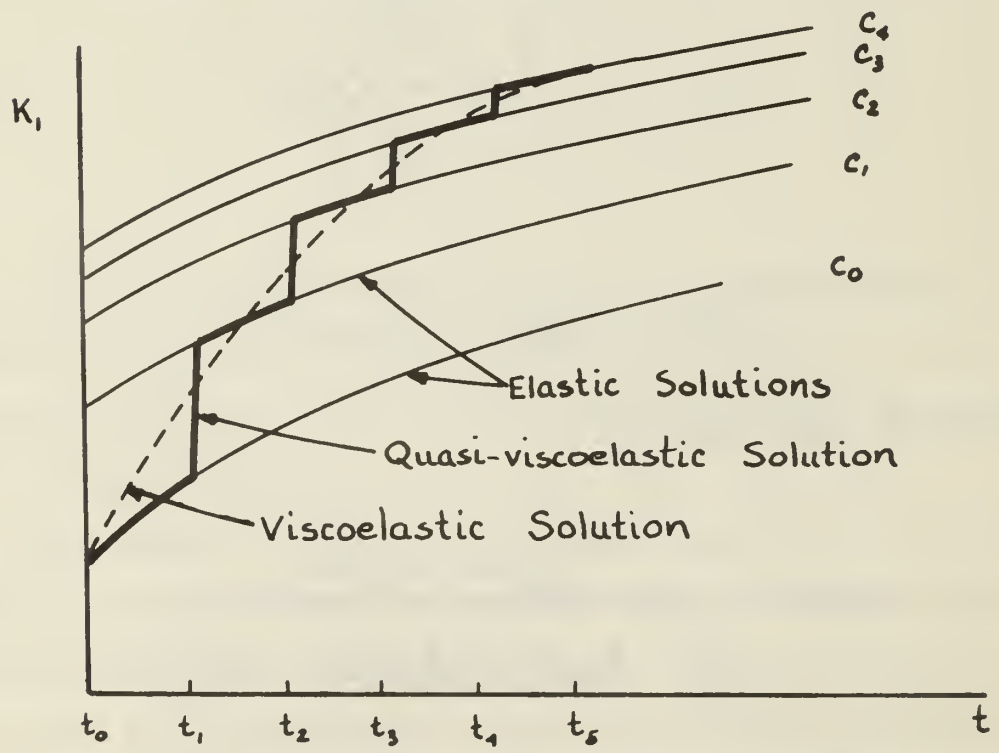

Fig. 24

Schmetic of Solution

Procedure

To illustrate how the solution should proceed, a step by step set of instructions will be given.

1. An appropriate time increment is selected and σ_r^v and σ_θ^v are computed for $p = p(t_1)$ and $E = E_{REL}(t_1)$ from Eqn. (I-19) for any given pressure-time trace. (r is taken to be $a + c_0$.) A time increment is selected by guess using estimates of load and resulting crack velocities as guidelines. The time increment should allow for moderate extension of the crack but not be so large that the accuracy of the solution is compromised.

2. Form $\sigma_r^v + \sigma_\theta^v$ and compute the equivalent modulus from Eqn. (69) for $t = t_1$ and $t = t_0$. In summation form it becomes,

$$E_{eq}(t_n) = \frac{\sigma_r^v(t_n) + \sigma_\theta^v(t_n)}{\sum_{i=0}^{n} D_{crp}(t_n - t_i)[(\sigma_r^v(t_i) + \sigma_\theta^v(t_i)) - \sigma_r^v(t_{i-1}) - \sigma_\theta^v(t_i - 1)]}$$

3. Knowing E_{eq}'s for the first time increment, λ_v's can be found for the corresponding times from Fig. 23.

4. Knowing λ_v from step 3 and σ_θ^v from step 1, compute $K_{ls}^v(t_1)$ from Eqn. (70) for the first time increment.

$$K_{ls}^v(t_n) = \sqrt{c_{n-1}} \sum_{i=0}^{n} \lambda_v(t_n - t_i)\, \sigma_\theta^v(t_i)\, \Delta t_i$$

5. Using the fracture characterization curve for the grain propellant (for example, see Fig. 17) find the crack velocity associated with the first time increment, c_0. Knowing the velocity and the length of the time increment, a new crack length, c_1, can be computed to be used for the next iteration.

6. Progress to $t = t_2$ and $c = c_1$ and find $\sigma_r^v(t_2)$ and $\sigma_\theta^v(t_2)$, using $p = p(t_2)$, $E = E_{REL}(t_2)$ and $r = a + c_1$ for the second time increment and values as before for t_1.
7. Compute E_{eq} for $t = t_2$, $t = t_1$, $t = t_0$.
8. Find corresponding λ_v's.
9. Compute $K_{ls}^v(t_2)$ and find the new crack velocity and crack length.
10. The process is repeated until the entire crack history is recorded as shown in Fig. 24.
11. From this information a crack history plot can be constructed as shown in Fig. 25.

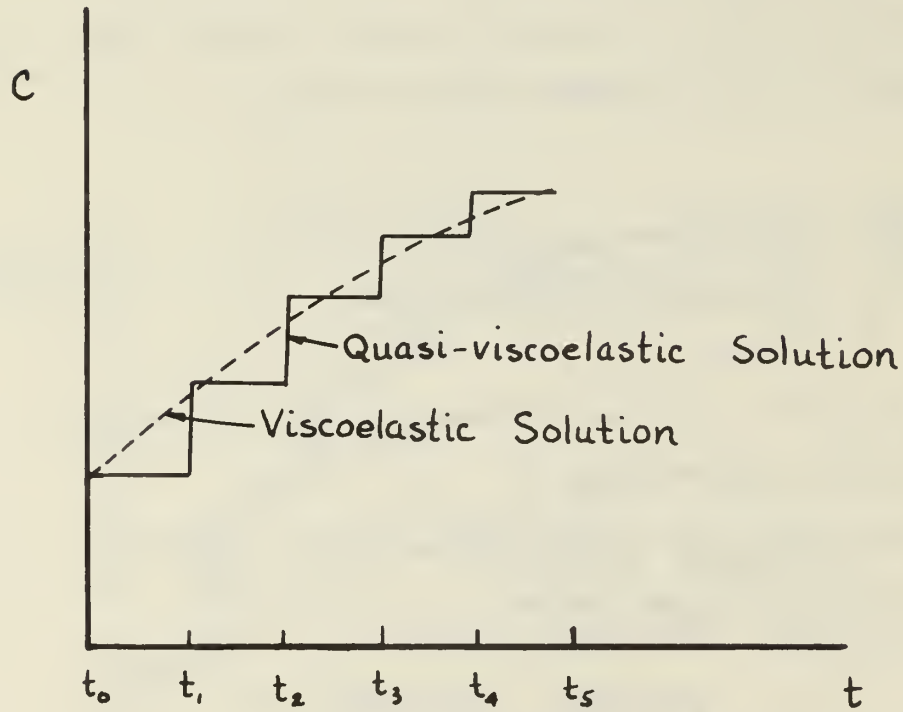

Fig. 25 Viscoelastic Crack History

This approximate solution is obtainable with realistic computer times and associated expenditures. At the same time it should yield good results.

SUMMARY AND CONCLUSIONS

The basic definitions for viscoelastic stress intensity factors are set forth with associated computations for determining them in laboratory specimens. Laboratory tests have been conducted to characterize propellants fracturewise, and the most suitable test found was the long strip subjected to a constant force loading. The influence of dewetting on the fracture characterization appears to be significant, but the matter has not yet been fully resolved.

An approximate method for performing viscoelastic fracture analyses has been presented which incorporates the fore-mentioned fracture characterization. It requires minimum computer usage and should yield good results.

APPENDIX I

An approximate method of viscoelastic analysis can be developed from linear superposition of elastic solutions. Such quasiviscoelastic solutions can give good solutions if properly used. The guidelines for use are formulated in this appendix by developing the quasiviscoelastic equations.

The elastic normal stress expressions for an encased circular cylinder are of the form

$$\sigma_{r,\theta e} = A_1 p' + B_1 p \qquad \text{(I-1)}$$

where p' is the interface pressure, and p is the bore pressure, A_1 and B_1 are functions of motor geometry and the radial coordinate; however they are not time dependent.

For σ_r ,

$$A_1 = \frac{-b^2}{b^2 - a^2}\left[1 - \frac{a^2}{r^2}\right] \qquad B_1 = \frac{a^2}{b^2 - a^2}\left[1 - \frac{b^2}{r^2}\right]$$

For σ_θ ,

$$A_1 = \frac{-b^2}{b^2 - a^2}\left[1 + \frac{a^2}{r^2}\right] \qquad B_1 = \frac{a^2}{b^2 - a^2}\left[1 + \frac{b^2}{r^2}\right]$$

From the elastic analysis,

$$p' = \frac{p}{A_2 + B_2 E} \qquad \text{(I-2)}$$

where A_2 and B_2 are composed of geometrical constants, and E is Young's Modulus of the propellant. The normal stress expression can then be written as

$$\sigma_{r,\theta e} = \frac{p}{A + BE} + B_1 p \qquad \text{(I-3)}$$

By the correspondence principle, the transformed stress for a unit step bore pressure is

$$\sigma^{v*}_{r,\theta I} = \frac{1/s}{A + BE^*} + \frac{B'}{s} \qquad \text{(I-4)}$$

where the asterisk indicates the Laplace Transform and $p^* = 1/s$. The subscript I on stress indicates the indicial stress response; i.e. the stress resulting from a unit step input loading.

For convenience in manipulation the first term in equation (I-2) will be designated σ_I^*.

$$\sigma_I^* = \frac{1/s}{A + BE^*} \qquad \text{(I-5)}$$

Clearing Equation (I-5) of fractions and inverting to the time plane,

$$A\sigma_I(t) + B\sigma_I(o)\, E_{REL}(t) + B \int_{o+}^{t} E_{REL}(t - \tau) \frac{d\sigma_I}{d\tau} d\tau = 1 \qquad \text{(I-6)}$$

If the integral is broken up into time increments for evaluation by summation, the expression (I-5) becomes

$$A\sigma_I(t) + B\sigma_I(o)\, E_{REL}(t) + B \sum_{i=1}^{n} E_{REL}(t - t_i)\, \Delta\sigma_{Ii} = 1 \qquad \text{(I-7)}$$

When $t = t_o = 0$, Equation (I-7) yields

$$\sigma_I(o) = \frac{1}{A + B\, E_{REL}(o)} \qquad \text{(I-8)}$$

This is the same as Equation (I-3) with E replaced by $E_{REL}(t)$.

Proceeding on in time to $t = t_1$, Equation (I-7) now becomes,

$$A\sigma_I(t_1) + B\sigma_I(o)\, E_{REL}(t_1) + B\, E_{REL}(o)\Delta\sigma_I(t_1) = 1 \qquad \text{(I-9)}$$

where

$$\Delta\sigma(t_1) = \sigma_1(t_1) - \sigma_I(o)$$

If $B\sigma_I(t_i)\, E_{REL}(t_1)$ is added and subtracted to Equation (I-9), it can be written in the form

$$[A + B\, E_{REL}(t_1)]\, \sigma_I(t_1) - B\Delta\, E_{REL}(t_1)\Delta\sigma_I(t_1) = 1 \qquad \text{(I-10)}$$

where

$$\Delta\, E_{REL}(t_1) = E_{REL}(t_1) - E_{REL}(o)$$

If $\Delta\, E_{REL}$ and $\Delta\sigma_I$ are chosen to be small compared to E_{REL} and σ_I in the numerical computing process,

$$\Delta\, E_{REL}(t_1) \doteq \frac{1}{A + B\, E_{REL}(t_1)} \qquad \text{(I-11)}$$

Once again this of the form of Equation (I-3) with E replaced by $E_{REL}(t_1)$. This procedure can be repeated for $t = t_2$; however more manipulating is required. The result is

$$[A + B\, E_{REL}(t_2)]\, \sigma_I(t_2) - B[\Delta\, E_{REL}(t_1)\, \Delta\, \sigma_I(t_2) + \Delta\, E_{REL}(t_2)\Delta\sigma_I(t_1)$$

$$+ \Delta\, E_{REL}(t_2)\, \Delta\sigma_I(t_2)] = 1 \qquad \text{(I-12)}$$

By the same criterion as before,

$$\sigma_I(t_2) \doteq \frac{1}{A + B\, E_{REL}(t_2)} \qquad \text{(I-13)}$$

It is assumed that this process can be repeated for an arbitrary number of time increments. As a result, a general relationship can be deduced

$$\sigma_I(t_i) \doteq \frac{1}{A + B\, E_{REL}(t_i)} \tag{I-14}$$

From equation (I-4) the viscoelastic stress components become upon inversion

$$\sigma^v_{r,\theta I}(t_i) \doteq \frac{1}{A + B\, E_{REL}(t_i)} + B_1 \tag{I-15}$$

Proceeding back one step further, the viscoelastic stress field resulting from a unit step in bore pressure is found from equation (I-3).

$$\sigma^v_{r,\theta I}(t_i) \doteq \left[\frac{\sigma_{r,\theta e}}{p} \right]_{E = E_{REL}(t_i)} \tag{I-16}$$

Since $\sigma_{r,\theta I}$ is the indicial response, the viscoelastic stress for an arbitrary pressure history can be obtained via the linear superposition integral.

$$\sigma^v_{r,\theta}(t) = \int_{o-}^{t} \sigma^v_{r,\theta I}(t-\tau) \frac{dp(\tau)}{d\tau}\, d\tau \tag{I-17}$$

In terms suited to numerical computation,

$$\sigma^v_{r,\theta}(t) = p(o)\sigma^v_{r,\theta I}(t) + \sum_{i=1}^{n} \sigma^v_{r,\theta I}(t-t_i)\Delta p_i \tag{I-18}$$

Relating this back to the elastic stress expression through equation (I-16),

$$\sigma^{v}_{r,\theta}(t) = p(o)\left[\frac{\sigma_{r,\theta e}}{p}\right]_{E=E_{REL}(t)} + \sum_{i=1}^{n}\left[\frac{\sigma_{r,\theta e}}{p}\right]_{E=E_{REL}(t-t_i)}\Delta p_i \quad \text{(I-19)}$$

The viscoelastic stress is obtained by subdividing the time into increments, determining the associated increments in applied pressure, Δp_i , and then appropriately summing.

REFERENCES

1. E. C. Francis, G. H. Lindsey and R. R. Parmerter, "Pressurized Crack Behavior in Two-Dimensional Rocket Motor Geometries," J. Spacecraft and Rockets, Vol. 9, No. 6, Jun. 1972, p. 415.
2. E. C. Francis, et. al., "Application of Fracture Mechanics to Predicting Failures in Solid Propellants," AFRPL-TR-70-105, Air Force Rocket Propulsion Laboratory, Edwards, California, Sep. 1970
3. W. G. Knauss, "Stable and Unstable Crack Growth in Viscoelastic Media," Trans. Society of Rheology, Vol. 13, No. 3, 1969, p. 291.
4. M. L. Williams, "On the Stress Distribution at the Base of a Stationary Crack," J. Applied Mechanics, Mar. 1957, p. 109.
5. H. M. Westergaard, "Bearing Pressures and Cracks," J. Applied Mechanics, Vol. 6, Trans. A.S.M.E., Vol. 61, 1939, p. A-49-A-53.
6. G. R. Irwin, "Analysis of Stresses and Strains Near the End of a Crack Traversing a Plate," J. Applied Mechanics, Sep. 1957, p. 361.
7. G. A. C. Graham, "Two Extending Crack Problems in Viscoelasticity Theory," Quarterly of Applied Mathematics, Vol. 27, No. 4, Jun. 1970, p. 497.
8. W. G. Knauss, "Delayed Failure--The Griffith Problem for Linearly Viscoelastic Materials," Int. J. of Fracture Mechanics, Vol. 6, No. 1, Mar. 1970, p. 7.
9. H. K. Meuller, "Stress Intensity Factor and Crack Opening for a Linearly Viscoelastic Strip with a Slowly Propagating Central Crack," Int. J. of Fracture Mechanics, Vol. 7, No. 2, Jun. 1971, p. 129.
10. H. K. Mueller and W. G. Knauss, "Crack Propagation in a Linearly Viscoelastic Strip," J. Applied Mechanics, Jun. 1971, p. 483.
11. G. A. C. Graham, "The Correspondence Principle of Linear Viscoelasticity Theory for Mixed Boundary Value Problems Involving Time-Dependent

Boundary Regions," Quarterly of Applied Mathematics, Vol. 26, 1968, p. 167.

12. W. G. Knauss, "Stresses in an Infinite Strip Containing a Semi-Infinite Crack," J. Applied Mechanics.

13. C. M. Hertzler, "Viscoelastic Fracture Characterization of a Solid Propellant," Naval Postgraduate School Thesis, Jun. 1972.

14. G. H. Lindsey and J. E. Wood, "An Isotropic Theory for Dewettable Solids," Naval Postgraduate School Report NPS-57Li71011A, Jan. 1971.

15. L. I. Deverall and G. H. Lindsey, "A Comparison of Numerical Methods for Determining Stress Intensity Factors," J. Basic Engineering, Jun. 1972, p. 508.

DISTRIBUTION LIST

		No. of Copies
1.	Arnold Adicoff Michaelson Laboratory Naval Weapons Center China Lake, California 93555	10
2	Defense Documentation Center Cameron Station Alexandria, Virginia 22314	20
3.	Library Naval Postgraduate School Monterey, California 93940	2
4.	Department of Aeronautics Naval Postgraduate School Monterey, California 93940	1
5.	Superintendent Naval Postgraduate School Monterey, California 93940	1
6.	G. H. Lindsey Associate Professor Department of Aeronautics Naval Postgraduate School Monterey, California 93940	5
7.	LT R. G. Kish Aero Engineering Programs Naval Postgraduate School Monterey, California 93940	1
8.	LT R. E. Kapernick Aero Engineering Programs Naval Postgraduate School Monterey, California 93940	1
9.	Eugene Francis United Technology Center 1050 East Arquez Avenue Sunnyvale, California 94086	1
10.	Harold Zitzer United Technology Center 1050 East Arquez Avenue Sunnyvale, California 94086	1

11. Dr. Lamar Deverall — 1
United Technology Center
1050 East Arquez Avenue
Sunnyvale, California 94086

12. Dr. S. A. Murch — 1
United Technology Center
1050 East Arquez Avenue
Sunnyvale, California 94086

13. Dr. John M. Wozencraft — 2
Dean of Research, Code 023
Naval Postgraduate School
Monterey, California 93940

DOCUMENT CONTROL DATA - R & D

Security classification of title, body of abstract and indexing annotation must be entered when the overall report is classified

ORIGINATING ACTIVITY (Corporate author)
Naval Postgraduate School
Monterey, California 93940

2a. REPORT SECURITY CLASSIFICATION
Unclassified

2b. GROUP

REPORT TITLE
Viscoelastic Analysis Method for Rocket Motors Containing Cracks

DESCRIPTIVE NOTES (Type of report and inclusive dates)
Technical Report NPS-57LI73031A

AUTHOR(S) (First name, middle initial, last name)
Gerald H. Lindsey

REPORT DATE	7a. TOTAL NO. OF PAGES	7b. NO. OF REFS
March 1973	58	15

8a. CONTRACT OR GRANT NO.	9a. ORIGINATOR'S REPORT NUMBER(S)
b. PROJECT NO.	
c.	9b. OTHER REPORT NO(S) (Any other numbers that may be assigned this report)
d.	

10. DISTRIBUTION STATEMENT

Approved for public release; distribution unlimited.

11. SUPPLEMENTARY NOTES	12. SPONSORING MILITARY ACTIVITY
	Naval Weapons Center China Lake, California 93555

13. ABSTRACT

The basic definitions for viscoelastic stress intensity factors are set forth with associated computations for determining them in laboratory specimens. Laboratory tests have been conducted to characterize propellants fracturewise, and the most suitable test found was the long strip subjected to a constant force loading. The influence of dewetting on the fracture characterization appears to be significant, but the matter has not yet been fully resolved.

An approximate method for performing viscoelastic fracture analyses has been presented which incorporates the fore-mentioned fracture characterization. It requires minimum computer usage and should yield good results.

14 KEY WORDS	LINK A		LINK B		LINK C	
	ROLE	WT	ROLE	WT	ROLE	WT
Viscoelastic						
Fracture						
Solid propellant						
Fracture characterization						
Crack propagation						